Mutations in the LKB1 tumour suppressor are frequently detected in tumours from Caucasian but not Asian lung cancer patients

JP Koivunen[1,2], J Kim[3,4], J Lee[3,4], AM Rogers[2], JO Park[1,2], X Zhao[2], K Naoki[2], I Okamoto[5], K Nakagawa[5], BY Yeap[6], M Meyerson[1,2,7,8,9], K-K Wong[1,2,9], WG Richards[10], DJ Sugarbaker[10], BE Johnson[1,2,9] and PA Jänne*[1,2,9]

[1]Lowe Center for Thoracic Oncology, Dana-Farber Cancer Institute, Boston, MA, USA; [2]Department of Medical Oncology, Dana-Farber Cancer Institute, Harvard Medical School, Boston, MA, USA; [3]Department of Thoracic Surgery, Samsung Medical Center, Seoul, Korea; [4]School of Medicine, Sungkyunkwan University, Seoul, Korea; [5]Department of Medical Oncology, School of Medicine, Kinki University, Osaka, Japan; [6]Department of Medicine, Massachusetts General Hospital, Boston, MA, USA; [7]Department of Pathology, Harvard Medical School, Boston, MA, USA; [8]The Broad Institute of MIT and Harvard Universities, Cambridge, MA, USA; [9]Department of Medicine, Brigham and Women's Hospital and Harvard Medical School, Boston, MA, USA; [10]Department of Surgery, Brigham and Women's Hospital, Boston, MA, USA

Somatic mutations of LKB1 tumour suppressor gene have been detected in human cancers including non-small cell lung cancer (NSCLC). The relationship between LKB1 mutations and clinicopathological characteristics and other common oncogene mutations in NSCLC is inadequately described. In this study we evaluated tumour specimens from 310 patients with NSCLC including those with adenocarcinoma, adenosquamous carcinoma, and squamous cell carcinoma histologies. Tumours were obtained from patients of US (n = 143) and Korean (n = 167) origin and screened for LKB1, KRAS, BRAF, and EGFR mutations using RT—PCR-based SURVEYOR-WAVE method followed by Sanger sequencing. We detected mutations in the LKB1 gene in 34 tumours (11%). LKB1 mutation frequency was higher in NSCLC tumours of US origin (17%) compared with 5% in NSCLCs of Korean origin (P = 0.001). They tended to occur more commonly in adenocarcinomas (13%) than in squamous cell carcinomas (5%) (P = 0.066). LKB1 mutations associated with smoking history (P = 0.007) and KRAS mutations (P = 0.042) were almost mutually exclusive with EGFR mutations (P = 0.002). The outcome of stages I and II NSCLC patients treated with surgery alone did not significantly differ based on LKB1 mutation status. Our study provides clinical and molecular characteristics of NSCLC, which harbour LKB1 mutations.
British Journal of Cancer (2008) 99, 245–252. doi:10.1038/sj.bjc.6604469 www.bjcancer.com
Published online 1 July 2008
© 2008 Cancer Research UK

Keywords: carcinoma; non-small cell lung; mutation; LKB1; EGFR; KRAS

Peutz–Jeghers syndrome (PJS) is caused by mutations in the LKB1 tumour suppressor gene (Hemminki et al, 1998). LKB1 is serine–threonine kinase, which has been shown to regulate cell cycle progression, apoptosis, and cell polarity (Tiainen et al, 1999). The major target of LKB1 kinase activity is thought to be AMP-activated protein kinase (AMPK). AMPK is activated under low cellular energy conditions by raising AMP levels and it phosphorylates multiple downstream targets including tubero-sclerosis complex 2 gene, which represses mTOR signalling. Phosphorylation of AMPK by LKB1 is needed for full activity of AMPK and suppression of mTOR activity under low energy conditions (Shaw et al, 2004). The hallmarks of PJS include mucocutaneous pigmentation and hamartomatous polyps of the gastrointestinal tract. Patients with PJS have an increased risk of developing gastrointestinal, pancreatic, breast, gynecological, and non-small cell lung cancers (NSCLC). The overall risk for cancers is increased 5- to 12-fold in different age groups compared with the general population (Hearle et al, 2006). Somatic mutations of the

*Correspondence: Dr PA Jänne, Lowe Center for Thoracic Oncology, Dana-Farber Cancer Institute, D820A, 44 Binney Street, Boston, MA 02115, USA; E-mail: pjanne@partners.org

LKB1 tumour suppressor have rarely been found in cancers from patients who do not have PJS except for NSCLC (Avizienyte et al, 1999). Previous reports have suggested the LKB1 mutation rate to be as high as 30% in NSCLC tumours and cell lines derived from patients of Caucasian origin (Carretero et al, 2004; Matsumoto et al, 2007) and to be infrequent in NSCLC patients of Asian origin (3%) (Onozato et al, 2007). Furthermore, LKB1 mutations have been shown to be associated with adenocarcinoma histology, male gender, and smoking history (Matsumoto et al, 2007). A recent report of using a mouse model for lkb1 inactivation in NSCLC has provided insights into the role of the gene in this cancer. This study showed that lkb1 inactivation in combination with activating mutations of kras using inducible promoters in the lung was associated with decreased survival compared with kras mutation alone (Ji et al, 2007).

Current screening techniques for LKB1 tumour suppressor mutations rely on conventional exonic sequencing of the DNA, which can identify single base pair changes and small deletions/insertions (Ballhausen and Gunther, 2003). The addition of multiple ligation-dependent probe amplification (MLPA), which enables detection of exonic and whole gene deletions, with exonic sequencing has increased the mutation detection rates to 80% in patients with PJS phenotype (Volikos et al, 2006). Conventional

sequencing has also been used to detect mutations of *LKB1* at mRNA level and some mutations missed by sequencing at the DNA level have been discovered by mRNA-based approaches (Abed *et al*, 2001). However, mutant forms of *LKB1* mRNAs can have a shortened half-life because of nonsense-mediated decay, which can potentially interfere with mutation detection (Abed *et al*, 2001).

We have recently described a rapid and sensitive enzymatic method to detect mutations in epidermal growth factor (*EGFR*) of DNA from fresh tissue and paraffin-embedded tissues (Janne *et al*, 2006). This method includes amplification of region of interest with PCR, SURVEYOR endonuclease digestion of the products, which cleaves mismatched heteroduplex DNAs, and detection of DNA fragments by sensitive high-performance liquid chromatography (HPLC) WAVE HS system. Subsequently, SURVEYOR-positive specimens are fractionated in partially denaturing conditions and are Sanger-sequenced. The major advantages of SURVEYOR-WAVE method are the fast exclusion of wild-type specimens without laborious conventional sequencing and high sensitivity. The SURVEYOR-WAVE method is more sensitive than conventional sequencing as it can detect mutant DNA sequences when they are present in 1% or more of total DNA (Janne *et al*, 2006).

The current study was designed to analyse the incidence of *LKB1* mutations in NSCLC. Furthermore, we wanted to investigate the *LKB1* mutational frequency in different histologies and ethnic backgrounds, and assess their correlation to smoking history, gender, stage, survival, and other oncogenic mutations in NSCLC.

MATERIALS AND METHODS

Cell lines and tumour specimens

The NSCLC cell lines A549, NCI-H1395, NCI-H1650, NCI-H1666, NCI-H1781, NCI-1975, NCI-H23, NCI-H2126, NCI-H441, NCI-H820, HCC2935, HCC4006, and HCC827 were purchased from ATCC (Manassas, VA, USA). H3255, H3255GR, HCC2279, and PC-9 have been previously described (Ono *et al*, 2004; Tracy *et al*, 2004; Engelman *et al*, 2006). Ma1, and Ma70 are NSCLC cell lines harbouring *EGFR* mutations that were established at the Kinki University, Osaka, Japan. A549, NCI-H1395, NCI-H1666, NCI-H23, NCI-H2122, NCI-H2126, and NCI-H460 have previously been reported to contain *LKB1* mutations (Sanchez-Cespedes *et al*, 2002; Bamford *et al*, 2004; Carretero *et al*, 2004).

NSCLC tumours (*n* = 310) were collected from surgical resections from patients with stages I–IV NSCLC when sufficient material for RNA extraction was available. The majority of the specimens (*n* = 167) was collected at the Samsung Medical Center, Seoul, Korea. Frozen tumour tissues were collected from 809 out of 2442 patients who underwent curative resection for NSCLC from November 1995 to February 2007 at Samsung Medical Center. One or two pieces from the periphery of the tumour masses – avoiding necrotic regions – were immediately frozen at −80°C until retrieved. Medical records and haematoxylin and eosin-stained slides of the specimen were reviewed by a single pathologist. Only frozen tumour tissues from adenocarcinoma or squamous cell carcinoma (according to the 2004 World Health Organization histopathological criteria) were included. Only frozen tumour tissues with a tumour cell content of more than 70% were used for further analysis. In addition, frozen tumour tissues of the following patients were excluded from the study: patients who had received preoperative neoadjuvant treatments, patients with double primary lung cancer, and patients who had undergone incomplete resections or who had not been subjected to mediastinal lymph node dissections. Selected frozen tumour tissues were used for the microdissection. Briefly, frozen tissues were lightly stained with haematoxylin – eosin to improve visualisation, and necrotic tumour tissues and intervening normal tissues were removed.

Each of the microdissected tumour tissues with a tumour cell content of more than 90% was placed in 1 ml Easy Blue reagent of a commercially available RNA isolation kit (easy-spin™ Total RNA Extraction Kit, iNtRON Biotechnology, Gyeonggi-do, Korea), immediately homogenised by vortexing, and the total RNA was extracted. The quantity and quality of RNA were analysed using a spectrometer (Nanodrop Technologies, Rockland, DE, USA) and Agilent 2100 Bioanalyzer (Agilent RNA 6000 Nano Kit, Agilent Technologies Inc., Böblingen, Germany), respectively. Finally, 167 frozen tissues with acceptable quality of RNA (RNA Integrity Number (RIN) value over 7.0) were used for the current studies. All patients provided written informed consent.

The tumours from Caucasian patients (*n* = 143) were collected at the Brigham and Women's Hospital, Boston, MA, USA between 1991 and 1997 and have been previously published for patient characteristics and histology, and for expression profile-based clustering of the tumours (Bhattacharjee *et al*, 2001; Hayes *et al*, 2006). Frozen samples of resected lung tumours were obtained within 30 min of resection and subdivided into 100 mg samples and snap frozen at −80°C. Each specimen was associated with an immediately adjacent sample embedded for histology in an optimal cutting temperature medium and stored at −80°C. Six micrometres of frozen sections of embedded samples stained with haematoxylin and eosin were used to confirm the postoperative pathological diagnosis and to estimate the cellular composition of adjacent samples. All specimens underwent pathological review by two pathologists. In all 109 tumours obtained during the same time period were excluded because they did not meet one or more of the eligibility criteria. Tissue samples were homogenised in Trizol (Life Technologies, Gaithersburg, MD, USA) and RNA was extracted and purified by using the RNeasy column purification kit (Qiagen, Chatsworth, CA, USA). Denaturing formaldehyde gel electrophoresis followed by northern blotting using a β-actin probe assessed RNA integrity. Samples were excluded if β-actin was not full length. All patients provided written informed consent. The US cohort included specimens that have previously undergone analyses and the results have been published for *EGFR*, *KRAS*, and *BRAF* mutations (Bhattacharjee *et al*, 2001; Naoki *et al*, 2002; Hayes *et al*, 2006). We reconfirmed the mutations in 30 of these specimens using the SURVEYOR-based analysis (see section SURVEYOR digestion and HPLC analysis) and found 100% concordance between the two methods (data not shown).

Cell line specimens were snap frozen and stored at −80°C. RNA was extracted from tumours and cell lines using Trizol (Invitrogen, Carlsbad, CA, USA), purified with Rneasy Mini Kit (Qiagen, Valencia, CA, USA) and was used for cDNA synthesis using the QuantiTect reverse transcription kit (Qiagen, Valencia, CA, USA).

PCR primers and cycling conditions

For *LKB1* gene analysis, PCR primers were designed to amplify the cDNA in two amplicons. PCR primers of the first amplicon were designed to hybridise to the noncoding area of the mRNA upstream of exon 1 (5′-agggaagtcggaacacaagg-3′) and to exon 5 (5′-ccagatgtccaccttgaagc-3′) generating a PCR product of 797 bp. The primers for the second amplicon located at exon 5 (5′-aacggcc tggacaccttct-3′) and to noncoding exon 10 (5′-gaaccggcaggaagact gag-3′) generating a product of 702 bp, which has an overlapping part with first amplicon. For SURVEYOR-WAVE analysis of *KRAS*, PCR primers (5′-ggcctgctgaaaatgactga-3′, 5′-tcctgagcctgttttgtgtct- 3′) were designed to generate an amplicon of 407 bp covering codons 12, 13 and 61, which are the codons commonly mutated in lung cancers. For SURVEYOR-WAVE mutation analysis of *BRAF*, cDNA was amplified in two overlapping amplicons (5′-aggattt cgtggtgatggag-3′, 5′-gatgacttctggtgccatcc-3′, and 5′-gacgggactcgagt gatgat-3′, 5′-ggtatcctcgtcccaccata-3′) covering codons 387 – 673. For SURVEYOR-WAVE analysis of *EGFR*, PCR amplification was done in a single amplicon (5′-ggagcctcttacacccagtg-3′,

5′-aggtcatcaactcccaaacg-3′), which covered exons 18–21 of the gene. PCR amplification was done using JumpStart Taq (Sigma, St Louis, MO, USA) under the manufacturer's guidelines. A part of the specimens ($n = 103$) was previously characterised for KRAS, BRAF, EGFR mutations using reverse transcritase (RT)–PCR and direct sequencing of the PCR products (Naoki et al, 2002; Hayes et al, 2006).

SURVEYOR digestion and HPLC analysis

SURVEYOR digestion and HPLC analysis were carried out as described previously (Janne et al, 2006). In brief, PCR products were digested in reaction mixture containing equal volumes of SURVEYOR enzyme (Transgenomics, Omaha, NE, USA) and Enhancer (Transgenomics, Omaha, NE, USA) at 42°C for 20 min followed by termination of the reaction by Stop Solution (Transgenomics, Omaha, NE, USA). Specimens were then loaded to the WAVE HS HPLC (Transgenomics, Omaha, NE, USA) at 50°C, eluted with an increasing acetonitrile gradient, and detected by UV detector using DNA intercalating fluorescence dye (Transgenomics, Omaha, NE, USA). When cell lines known to be homozygous for specific mutation were analysed, PCR products were mixed 1:1 with PCR products of a wild-type cell line, denatured by heating, and slowly renatured to generate heteroduplexes.

Sequencing and fractionation

Specimens that showed an altered pattern on the SURVEYOR tracings were purified using QIAquick kit (Qiagen, Valencia, CA, USA) and sequenced bi-directionally by molecular biology core facility of Dana–Farber Cancer Institute. If a specimen showed an altered pattern on the SURVEYOR tracing but had a wild-type sequence by direct DNA sequencing, it underwent fractionation by WAVE HS HPLC in partially denaturing conditions. Running temperatures for specific amplicons were calculated by the Navigator Software (Transgenomics, Omaha, NE, USA). Collected fragments were amplified with PCR using the same primers as in the original amplification, purified and sequenced as previously described above.

Statistical analysis

Fisher's exact test was used to assess the association of LKB1 mutation status with other clinical, pathological, and genetic characteristics. To adjust for any difference between ethnic groups, the association between LKB1 mutation rate and each characteristic was also evaluated as stratified contingency tables. If we did not reject that the odds ratios were the same across ethnic groups, we then tested whether the common odds ratios were unity based on the stratified Mantel–Haenszel estimate (Breslow and Day, 1980). Overall survival was estimated using the Kaplan–Meier method, with differences between the groups compared using the log-rank test. All P-values were based on a two-sided hypothesis, with $P < 0.05$ considered to be statistically significant and $0.05 < P < 0.10$ considered to be borderline significant.

RESULTS

SURVEYOR-WAVE mutation detection of LKB1 tumour suppressor in NSCLC cell lines

The impact of the stability of LKB1 mRNA on detecting LKB1 mutations was tested using RT–PCR with mRNA extracted from NSCLC cell lines that had previously been characterised for LKB1 mutations. These included NCI-H441 (wild type) and A549, NCI-H1395, NCI-H23, and NCI-H2126 (all containing LKB1 mutations). Reverse transcriptase–PCR amplification of the whole coding

region of the LKB1 mRNA showed that cell lines with nonsense (A549, NCI-H23) mutations or 1 bp deletion (H1395) expressed mRNA with comparable size to the wild-type H441 cell line (1460 bp). H2126 cell line, which is known to have homozygous deletion of exons 4–6, expressed mRNA with substantially smaller size (~1000 bp) corresponding to deletion of 398 bp. RT–PCR revealed no major difference in LKB1 mRNA expression levels between LKB1 mutant or wild-type cell lines (Figure 1A).

As LKB1 mutant and wild-type cell lines expressed comparable amounts of LKB1 mRNA with RT–PCR, we studied the cDNA for mutations using the SURVEYOR-WAVE method. The WAVE HPLC provides a system to analyse DNA fragments smaller than 900 bp and therefore we designed two overlapping amplicons covering exons 1–5 (797 bp) and 5–9 (702 bp) to amplify the whole coding region of LKB1 mRNA. PCR products of LKB1 mutant cell lines were mixed 1:1 with the products from wild-type cell lines (H441) to generate heteroduplexes as LKB1 mutant cell lines were previously reported to be homozygous for the inactivation of the gene. SURVEYOR-WAVE analysis of the amplicon covering exons 1–5 revealed novel peaks with the cDNA for A549, and NCI-H1395 cell lines compared with the wild type from NCI-H441 (Figure 1B). SURVEYOR-WAVE analysis of exons 5–9 showed novel peaks for the NCI-H23 cell line as well. The mutations detected with SURVEOR-WAVE were confirmed by conventional DNA sequencing and they corresponded to previous reports (Sanchez-Cespedes et al, 2002; Carretero et al, 2004). We could not detect the LKB1 mutation of H2126 cell line with SURVEYOR-WAVE method using a two-amplicon approach because this cell line has a homozygous deletion of exons 4–6 and the reverse primer of the first amplicon and the forward primer of the second amplicon, which lie on the deleted part of the gene (data not shown).

LKB1 tumour suppressor gene mutations in NSCLC tumours

We next used the SURVEYOR-WAVE method to screen NSCLC tumour specimens ($n = 310$) for LKB1 mutations. We detected 34 LKB1 mutations (11%) in the NSCLC tumour specimens (Table 1). The majority of the LKB1 mutations detected was deletions or insertions ($n = 25$, 74%). The remainder was missense ($n = 7$, 21%) and nonsense ($n = 2$, 6%) mutations (Table 2, Figure 1C). About one-half of the deletions and insertions were small, covering <15 bp ($n = 14$, 56%), whereas larger deletions ($n = 11$, 44%) covering hundreds of base pairs were detected in the remaining specimens. Some mutational hotspots were discovered. The areas that had the same mutation in more than one tumour specimen included deletion of exon 4 ($n = 4$), deletion of exons 2 and 3 ($n = 3$), D194Y ($n = 2$), and P281L ($n = 2$). Interestingly, a significant portion of the mutations was located in exon 1 ($n = 11$, 32%) but there was no area of recurrent mutations in this exon (Table 2). Of the missense mutations detected in the current study, all except R426W are in the kinase domain of the protein. Missense mutations in codons 176 and 194 have been previously characterised in PJS (Launonen, 2005). We also found four F354L alterations (data not shown) but we did not consider these as missense mutations as this alteration has previously been reported to be a rare polymorphism of the gene (Launonen et al, 2000). We did not have access to the corresponding normal tissues and therefore, we could not verify if some of the missense mutations were somatic or germline.

Association of LKB1 tumour suppressor mutations in NSCLC with clinicopathological characteristics

The mutation frequency of LKB1 gene was significantly higher in NSCLCs in the Caucasian cohort (Table 1). Twenty-five (17% of specimens) of the LKB1 mutations were detected in NSCLCs
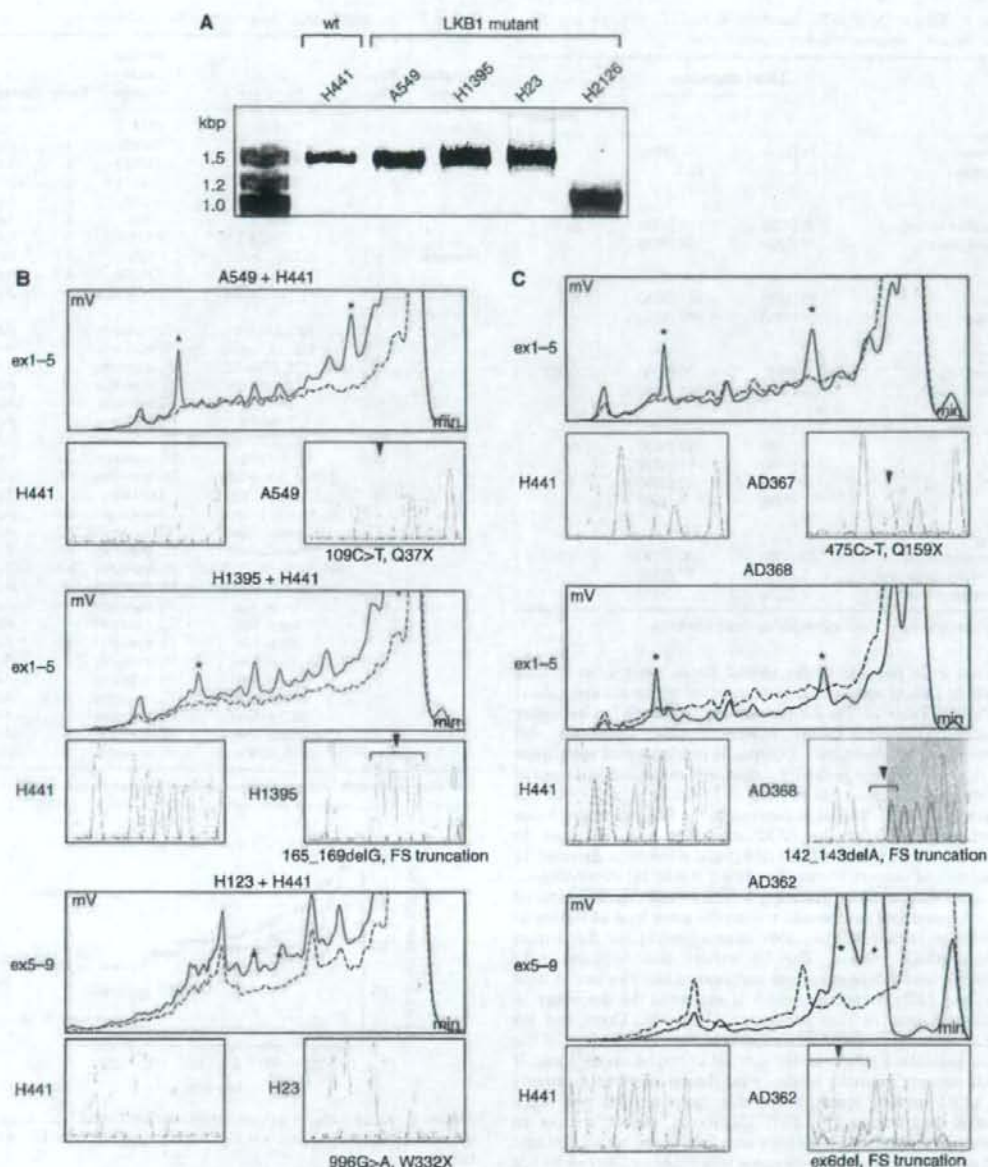
358

Figure 1 Mutation analysis of *LKB1* gene in NSCLC cell lines and tumours. RT–PCR amplification of cDNA from *LKB1* wt (H441) and *LKB1* mutant (A549, H1395, and H23) cell lines display the full length LKB1 mRNA (1.4 kbp) while the *LKB1* mutant cell line, H2126 with a deletion of exons 4–6 expresses a shorter mRNA (1.0 kbp) (**A**). HPLC tracings of SURVEYOR-WAVE mutation analysis of NSCLC cell lines A549, H1395, or H23 (continuous line), and H441 (dashed line). Time in minutes is shown on the X-axis, voltage in mV on the Y-axis (**B**). A549 and H1395 show novel peaks (*) in the amplicon covering exons 1–5 (ex1–5) corresponding to 109C>T, Q37X and 165_169delG, frameshift and truncation (FS truncation) mutations. The analysis from H23 demonstrates novel peaks in the amplicon covering exons 5–9 (ex5–9) corresponding to 996G>T, W332X mutation. *LKB1* wild-type cDNA (H441) was added to PCR products 1:1, denatured by heating and slowly renaturated to generate heteroduplexes since A549, H1395, and H23 have previously reported to be homozygous for the *LKB1* mutations. SURVEYOR-WAVE mutation analyses of NSCLC tumours (**C**). AD367 and AD368 tumours showed novel peaks in the ex1–5 amplicon corresponding to 475C>T, Q159X, and 142_143delA, FS, truncation mutations. AD362 tumour had novel peaks in ex5–9 amplicon corresponding to deletion of exon 6. Mutant sequences for AD367 and AD368 are displayed from sequences using the forward primer while mutation of the AD362 is showed with reverse primer.

Table 1 Frequency of *LKB1* mutations in NSCLC tumours and their association with clinicopathological characteristics

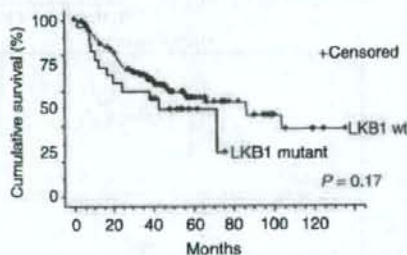|	LKB1 mutation		
	+	–	P-value*
All tumours	34 (11%)	276 (89%)	
Age, median	61.2	62.2	
Ethnicity			
Caucasian cohort	25 (17%)	118 (83%)	0.001
Asian cohort	9 (5%)	158 (95%)	
Gender			
Male	20 (11%)	167 (89%)	NS
Female	14 (12%)	107 (88%)	
Smoking			
Never (<10 py)	2 (3%)	70 (97%)	0.007
Smoker (>10 py)	26 (14%)	161 (86%)	
Tumour stage			
I	19 (10%)	169 (90%)	NS
II	8 (14%)	51 (86%)	
III	5 (11%)	42 (89%)	
IV	1 (12%)	7 (88%)	
Histology			
Adenocarcinoma	27 (13%)	180 (87%)	0.047
Squamous carcinoma	5 (5%)	87 (95%)	
Adenosquamous	2 (22%)	7 (78%)	

*Fisher's exact test. NS = not statistically significant (P > 0.05).

collected from patients in the United States, whereas only nine mutations (5% of specimens) were detected in the Korean cohort (P = 0.001) (Table 1). The *LKB1* mutation rate tended to be higher in adenocarcinomas (13%) compared with squamous cell carcinomas (5%) (P = 0.067). Differences in histological subgroups were relatively modest in the US cohort with mutations in 18 out of 94 (19%) adenocarcinomas *vs* 5 out of 38 (13%) in squamous cell cancers (P = 0.461). This is in contrast to the findings in the Asian patients where all of the *LKB1* mutations were detected in adenocarcinomas (9 out of 113 (8%)) and none were detected in squamous cell cancers (0 out of 54 (0%); P = 0.032). Nevertheless, the higher rate of *LKB1* mutation in adenocarcinomas compared with squamous cell carcinomas retains the same level of statistical significance (stratified P = 0.064) after adjusting for fluctuation between ethnic groups. The US cohort also included nine specimens from adenosquamous carcinomas and two out of nine (22%) had *LKB1* mutations, which is similar to the frequency in adenocarcinomas in this population (Table 1). There was no association between *LKB1* mutations and the clinical stage of the NSCLC patients. Kaplan–Meier survival curves of stages I and II NSCLC patients showed a tendency for shorter survival in patients with *LKB1* mutant tumours but this, however, did not reach statistical significance (P = 0.17) (Figure 2). No differences in survival were observed in patients who harboured both *LKB1* and *KRAS* mutations compared with those with *KRAS* or *LKB1* alone but the total number of patients with both mutations who had stages I or II NSCLC was small (n = 9; data not shown). We detected an association of *LKB1* mutations with a smoking history (P = 0.007) and only two mutations were detected in tumours from 72 NSCLC patients who were either never or light (⩽10 pack years) former smokers (Table 1). After adjusting for ethnic group, the higher rate of *LKB1* mutation among patients with a smoking history is borderline significant (stratified P = 0.067). The reduction in statistical significance is likely owing to the loss of power associated with the overall rarity of *LKB1* mutations among never or light former smokers. For these analyses we combined both never

Table 2 The specific *LKB1* mutations in NSCLC tumours

Mutation type	No. (%)	Mutation	Amino acid change	Exon	Histology
Missense	7 (21)	ª526G>T	D176Y	4	Ad
		ª580G>T	D194Y	4	Ad
		580G>T	D194Y	4	Sq
		829G>T	D277Y	6	AdSq
		ª842C>T	P281L	6	Ad
		ª842C>T	P281L	6	Ad
		1276C>T	R426W	9	Ad
Nonsense	2 (6)	206C>A	S69X	1	Ad
		475C>T	Q159X	4	Ad
Deletion/ insertion	25 (74)	ª75_76del2&insT	FS, truncates	1	Ad
		120_130del11	FS, truncates	1	Ad
		125_127insGG	FS, truncates	1	Ad
		128_129delC	FS, truncates	1	Ad
		142_143delA	FS, truncates	1	Ad
		180delC	FS, truncates	1	Ad
		209delA	FS, truncates	1	Ad
		227_228delC	FS, truncates	1	Ad
		47_651del604	FS, truncates	1-5	Sq
		153_536del384	FS, truncates	1-4	AdSq
		ªexon 2-3del	Truncates	2-3	Sq
		ªexon 2-3del	Truncates	2-3	Ad
		exon 2-3del	Truncates	2-3	Ad
		exon 2-4del	FS, truncates	2-4	Sq
		464_465del2insTTTGCT	FS, truncates	3-4	Sq
		562_563delG	FS, truncates	4	Ad
		ªexon 4del	FS, truncates	4	Ad
		exon 4del	FS, truncates	4	Ad
		exon 4del	FS, truncates	4	Ad
		610_623del14	FS, truncates	5	Ad
		ª837_844delC	FS, truncates	6	Ad
		837_844insC	FS, truncates	6	Ad
		exon 6del	FS, truncates	6	Ad
		1038_1040insG	FS, truncates	8	Ad

Ad = Adenocarcinoma; AdSq = Adenosquamous carcinoma; Sq = Squamous cell carcinoma; . ªThese mutations were detected in Korean NSCLC patients.

Figure 2 Kaplan–Meyer survival curves of stage I and II NSCLC patients with LKB1 wildtype (red line, n = 198) vs LKB1 mutant (blue line, n = 23) tumours.

smokers and light (⩽10 pack years) smokers as the frequency of mutations in other oncogenes such as *EGFR* is similar in these two patient groups (Pham *et al*, 2006). There were no correlations between *LKB1* mutations and gender or age of a patient.

Association of *LKB1* mutations with *K-Ras*, *B-Raf*, and *EGFR* mutations in NSCLC

Previous reports have suggested that in NSCLC cell lines, *LKB1* mutations often occur concurrently with *KRAS* or *BRAF* mutations

(Sanchez-Cespedes *et al*, 2002; Carretero *et al*, 2004). Furthermore, *EGFR* mutations are often mutually exclusive with *KRAS* mutations in NSCLC (Kosaka *et al*, 2004; Marchetti *et al*, 2005). We used combined data from previous papers (Sanchez-Cespedes *et al*, 2002; Carretero *et al*, 2004) and from Sanger institute's databases (Bamford *et al*, 2004) to analyse association of *LKB1* mutations with mutations of *KRAS*, *BRAF*, and *EGFR*. Analysis of *LKB1* mutation harbouring NSCLC cell lines (A-427, A549, NCI-H1395, NCI-H1666, NCI-H2122, NCI-H2126, NCI-H23, and NCI-H460) showed that five of the cell lines (63%) had concurrent *LKB1* and *KRAS* mutations, two (25%) had concurrent *LKB1* and *BRAF* mutations, and only one (13%) had neither *KRAS* nor *BRAF* mutations. None of these cell lines had EGFR mutations.

As our findings in NSCLC cell lines suggested concurrency of *KRAS* or *BRAF* and mutual exclusiveness of *EGFR* mutations with *LKB1* mutations, we analysed the mutational status of these genes in our primary NSCLC tumour specimens. *KRAS* mutations were detected in 49 (16% in the whole tumour set, 25% in Caucasian, and 8% in Asian specimens) tumour specimens with 10 (20% of *KRAS* mutants) of these occurring concurrently with an *LKB1* mutation (*P* = 0.042) (Table 3). Four *BRAF* mutations (1%) were found in the tumour set (G465V, N581S, L596R, and T599I) and one of these (N581S) occurred concurrently with *LKB1* mutation (*P* = 0.373). Seventy tumours (23% in the whole tumour set, 9% in Caucasian, 34% in Asian specimens) had *EGFR* kinase domain mutations with only one of them occurring concurrently with an *LKB1* mutation (*P* = 0.002). The tumour with a concurrent *EGFR* and *LKB1* mutation had a missense mutation of *LKB1* outside the kinase domain (R426W). No germ line DNA was available from this patient. However, a recent report has suggested that R426W is in fact a rare polymorphism of the gene (Onozato *et al*, 2007). Taken

Table 3 Association of *LKBI* mutations with *KRAS*, *BRAF*, and *EGFR* mutations in NSCLC tumours

| | | LKBI mutation | | |
		+	–	P-value*
EGFR mutation	+	1	69	0.002
	–	33	207	
K-Ras mutation	+	10	39	0.042
	–	24	237	
B-Raf mutation	+	1	3	0.373
	–	33	273	

*Fisher's exact test.

Table 4 *LKBI* genotypes of NSCLC cell lines with EGFR or ERBB2 mutations

Cell line	EGFR genotype	HER2 genotype	LKBI genotype
H1650	E746_A750del	Wt	Wt
H1781	Wt	G776V, Cins	Wt
H1975	L858R, T790M	Wt	Wt
H3255	L858R	Wt	Wt
H3255GR	L858R, T790M	Wt	Wt
H820	L747_L751del, T790M	Wt	Wt
HCC2279	E746_A750del	Wt	Wt
HCC2935	E746_T751del, S752I	Wt	Wt
HCC4006	L747_E749del, A750P	Wt	Wt
HCC827	E746_A750del	Wt	Wt
Ma-1	E746_A750del	Wt	Wt
Ma-70	L858R	Wt	Wt
PC-9	E746_A750del	Wt	Wt

Wt = wild type.

together our findings suggest that unlike *KRAS*, mutations in *EGFR* and *LKB1* are mutually exclusive in NSCLC.

Previous reports (Sanchez-Cespedes *et al*, 2002; Carretero *et al*, 2004) and Cancer Genome Project by Sanger Institute (Bamford *et al*, 2004) have extensively characterised *LKB1* mutations in NSCLC cell lines with *KRAS* and *BRAF* mutations, but *LKB1* status of *EGFR* mutant NSCLC cell lines has not been extensively analysed. Therefore, we analysed the *LKB1* genotype of NSCLC cell lines with known *EGFR* or *ERBB2* mutations. Twelve *EGFR* mutant and one *ERBB2* mutant cell lines were analysed for *LKB1* genotype. No *LKB1* mutations were detected in these cell lines (Table 4).

DISCUSSION

The present study characterised *LKB1* mutation frequency in NSCLC using one of the largest tumour sets to date (*n* = 310). Our study analysed tumours from different histologies and of both a US and Korean origin to determine potential histological and ethnic variation in *LKB1* mutational frequency. The large size of our study enabled us to study associations of *LKB1* mutations with clinocopathological factors, which have been incompletely characterised in previous studies (Sanchez-Cespedes *et al*, 2002; Carretero *et al*, 2004; Fernandez *et al*, 2004; Matsumoto *et al*, 2007; Onozato *et al*, 2007). In addition, we used a modification of a sensitive mutation screening technique that we have previously developed to facilitate the rapid detection of *LKB1* mutations (Janne *et al*, 2006).

Findings from our study confirm the high frequency of *LKB1* mutations in NSCLC (11%), which in contrast, are rare (0–4%) in other common solid malignancies (Avizienyte *et al*, 1998, 1999). The reason behind these observations is presently unknown but might reflect the differences in carcinogen exposure in the lungs compared with other tissues. In support of this hypothesis, we find that *LKB1* mutations are significantly (*P* = 0.007) more common in smokers than in never or light (⩽10 pack years) cigarette smokers (Table 1). Male PJS patients (age ⩾50 years) have an increased risk of developing lung cancer compared with the general population but the relationship of smoking and the increased risk of lung cancer in PJS is unknown (Hearle *et al*, 2006). Interestingly, the *LKB1* mutation spectrum found in the current study is very similar to those previously published for PJS (deletions 34%, insertions 15%, splice site mutations 14%, missense mutations 21%, and nonsense mutations 12%) (Launonen, 2005) and, as in PJS, no clear mutational hotspots were detected.

Our study also demonstrated that the *LKB1* mutation frequency was significantly higher in cancers derived from a US population compared with those found in Korean patients (17 vs 5%; *P* = 0.001). These differences also track with cigarette smoking, as the number of never/light former smokers was much higher in the Korean cohort compared with the US cohort of patients (38 vs 13%). Similarly, a recent study of 100 Japanese NSCLCs found that only 3% contained an *LKB1* mutation (Onozato *et al*, 2007). These findings are in contrast to *EGFR* mutations, which are more frequently detected in tumours from never/light cigarette smokers and from Asian patients (Janne and Johnson, 2006). Our studies further highlight ethnic and environmental differences in the origins of NSCLC.

Given the differences in *LKB1* mutation frequencies in smokers vs never/light smokers and in the US compared with Korean patients, we further determined whether these were also associated with other oncogene mutations known to vary in these subgroups of patients. Consistent with prior studies we found a significant association with concurrent *KRAS* mutations, which are common in smokers (Ahrendt *et al*, 2001), in one out of three of NSCLC with *LKB1* mutations (Table 3). In contrast, there was a significant inverse relationship of *LKB1* mutations with *EGFR* mutations in both NSCLC tumours and cell lines, which has not previously been

Clinical Studies

described (Tables 3 and 4). These differences may relate to the biological role of LKB1 in lung cancer. It is possible that in EGFR mutant lung cancers there is already maximal activation of the PI3K/Akt/mTOR signalling pathway and thus an LKB1 mutation may not be required to further potentiate this signalling pathway. In contrast in KRAS mutant cancers, a concurrent LKB1 mutation may be required to enhance mTOR activation. Mice with concurrent KRAS mutations and LKB1 inactivation have more aggressive tumours and a shorter survival than those with only KRAS mutant cancers (Ji et al, 2007). In our study, we were not able to detect a significant survival difference for patients whose tumours contained LKB1 mutations alone or concurrently with KRAS mutations (data not shown) likely because of the limited number of tumour specimens. Additional studies are needed to clarify the prognostic impact of LKB1 mutations in humans with NSCLC. In the present study ~2 out of 3 of LKB1 mutant tumours were KRAS wild type (Table 3). One possibility is that such tumours contain a concurrent mutation in another oncogene that activates the same signalling pathway as KRAS. For this reason, we examined our tumours for BRAF mutations, which are found in 1–2% of NSCLC (Naoki et al, 2002). We detected a concurrent LKB1 mutation in one of the four BRAF mutant tumours (Table 3). This tumour was wild type for KRAS (data not shown). In addition, some of the BRAF mutant NSCLC cell lines (NCI-H1395, G469A; NCI-H1666, G466V) also contain a concurrent LKB1 mutation (Sanchez-Cespedes et al, 2002; Bamford et al, 2004; Carretero et al, 2004). Future studies will help further clarify whether LKB1 mutations occur concurrently with other genomic alterations in NSCLC and the impact of this on patient outcome.

Our study employed a mutation scanning technology to screen for LKB1 mutations at the cDNA level (Janne et al, 2006). This was advantageous as the entire coding region of LKB1 could be rapidly screened for a mutation using just two overlapping cDNA fragments. LKB1 is a challenging gene to analyse at the genomic DNA level because of its high guanine–cytosine content. In addition, as many of the LKB1 mutations are small deletions (Table 2) or involve deletions of entire exons, these would be missed using exon-specific genome sequencing methods. Our method, however, does have limitations as it would miss deletions at the site of PCR primers, whole gene deletions, or deletions within the promoter region all of which have been infrequently detected in PJS (Volikos et al, 2006). Thus our studies may underestimate the true LKB1 mutation frequency in NSCLC. In addition, our method is limited to the analysis of fresh tumour specimens, which are available only from the minority of NSCLC patients. Furthermore, as techniques isolating mRNA from formalin-fixed paraffin-embedded tumour specimens continue to improve, this rapid mutation scanning technique can be used to analyse broader populations of tumours from NSCLC patients. Future studies may need to employ a combination of LKB1 mutation detection methodologies including the current method, MLPA and direct sequencing.

ACKNOWLEDGEMENTS

REFERENCES

Abed AA, Gunther K, Kraus C, Hohenberger W, Ballhausen WG (2001) Mutation screening at the RNA level of the STK11/LKB1 gene in Peutz-Jeghers syndrome reveals complex splicing abnormalities and a novel mRNA isoform (STK11 c.597(insertion mark)598insIVS4). Hum Mutat 18: 397–410

Ahrendt SA, Decker PA, Alawi EA, Zhu Yr YR, Sanchez-Cespedes M, Yang SC, Haasler GB, Kajdacsy-Balla A, Demeure MJ, Sidransky D (2001) Cigarette smoking is strongly associated with mutation of the K-ras gene in patients with primary adenocarcinoma of the lung. Cancer 92: 1525–1530

Avizienyte E, Loukola A, Roth S, Hemminki A, Tarkkanen M, Salovaara R, Arola J, Butzow R, Husgafvel-Pursiainen K, Kokkola A, Jarvinen H, Aaltonen LA (1999) LKB1 somatic mutations in sporadic tumors. Am J Pathol 154: 677–681

Avizienyte E, Roth S, Loukola A, Hemminki A, Lothe RA, Stenwig AE, Fossa SD, Salovaara R, Aaltonen LA (1998) Somatic mutations in LKB1 are rare in sporadic colorectal and testicular tumors. Cancer Res 58: 2087–2090

Ballhausen WG, Gunther K (2003) Genetic screening for Peutz-Jeghers syndrome. Expert Rev Mol Diagn 3: 471–479

Bamford S, Dawson E, Forbes S, Clements J, Pettett R, Dogan A, Flanagan A, Teague J, Futreal PA, Stratton MR, Wooster R (2004) The COSMIC (Catalogue of Somatic Mutations in Cancer) database and website. Br J Cancer 91: 355–358

Bhattacharjee A, Richards WG, Staunton J, Li C, Monti S, Vasa P, Ladd C, Beheshti J, Bueno R, Gillette M, Loda M, Weber G, Mark EJ, Lander ES, Wong W, Johnson BE, Golub TR, Sugarbaker DJ, Meyerson M (2001) Classification of human lung carcinomas by mRNA expression profiling reveals distinct adenocarcinoma subclasses. Proc Natl Acad Sci USA 98: 13790–13795

Breslow NE, Day NE, International Agency for Research on Cancer (1980) Statistical methods in cancer research. Vol. 1. Analysis of case–control studies. IARC scientific publications; no. 32. International Agency for Research on Cancer: Lyon

Carretero J, Medina PP, Pio R, Montuenga LM, Sanchez-Cespedes M (2004) Novel and natural knockout lung cancer cell lines for the LKB1/STK11 tumor suppressor gene. Oncogene 23: 4037–4040

Engelman JA, Mukohara T, Zejnullahu K, Lifshits E, Borras AM, Gale CM, Naumov GN, Yeap BY, Jarrell E, Sun J, Tracy S, Zhao X, Heymach JV, Johnson BE, Cantley LC, Janne PA (2006) Allelic dilution obscures detection of a biologically significant resistance mutation in EGFR-amplified lung cancer. J Clin Invest 116: 2695–2706

Fernandez P, Carretero J, Medina PP, Jimenez AI, Rodriguez-Perales S, Paz MF, Cigudosa JC, Esteller M, Lombardia L, Morente M, Sanchez-Verde L, Sotelo T, Sanchez-Cespedes M (2004) Distinctive gene expression of human lung adenocarcinomas carrying LKB1 mutations. Oncogene 23: 5084–5091

Hayes DN, Monti S, Parmigiani G, Gilks CB, Naoki K, Bhattacharjee A, Socinski MA, Perou C, Meyerson M (2006) Gene expression profiling reveals reproducible human lung adenocarcinoma subtypes in multiple independent patient cohorts. J Clin Oncol 24: 5079–5090

Hearle N, Schumacher V, Menko FH, Olschwang S, Boardman LA, Gille JJ, Keller JJ, Westerman AM, Scott RJ, Lim W, Trimbath JD, Giardiello FM, Gruber SB, Offerhaus GJ, de Rooij FW, Wilson JH, Hansmann A, Moslein G, Royer-Pokora B, Vogel T, Phillips RK, Spigelman AD, Houlston RS (2006) Frequency and spectrum of cancers in the Peutz-Jeghers syndrome. Clin Cancer Res 12: 3209–3215

Hemminki A, Markie D, Tomlinson I, Avizienyte E, Roth S, Loukola A, Bignell G, Warren W, Aminoff M, Hoglund P, Jarvinen H, Kristo P, Pelin K, Ridanpaa M, Salovaara R, Toro T, Bodmer W, Olschwang S, Olsen AS, Stratton MR, de la Chapelle A, Aaltonen LA (1998) A serine/threonine kinase gene defective in Peutz-Jeghers syndrome. Nature 391: 184–187

Janne PA, Borras AM, Kuang Y, Rogers AM, Joshi VA, Liyanage H, Lindeman N, Lee JC, Halmos B, Maher EA, Distel RJ, Meyerson M, Johnson BE (2006) A rapid and sensitive enzymatic method for epidermal growth factor receptor mutation screening. Clin Cancer Res 12: 751–758

Janne PA, Johnson BE (2006) Effect of epidermal growth factor receptor tyrosine kinase domain mutations on the outcome of patients with non-small cell lung cancer treated with epidermal growth factor receptor tyrosine kinase inhibitors. *Clin Cancer Res* 12: 4416s–4420s

Ji H, Ramsey MR, Hayes DN, Fan C, McNamara K, Kozlowski P, Torrice C, Wu MC, Shimamura T, Perera SA, Liang MC, Cai D, Naumov GN, Bao L, Contreras CM, Li D, Chen L, Krishnamurthy J, Koivunen J, Chirieac LR, Padera RF, Bronson RT, Lindeman NI, Christiani DC, Lin X, Shapiro GI, Janne PA, Johnson BE, Meyerson M, Kwiatkowski DJ, Castrillon DH, Bardeesy N, Sharpless NE, Wong KK (2007) LKB1 modulates lung cancer differentiation and metastasis. *Nature* 448: 807–810

Kosaka T, Yatabe Y, Endoh H, Kuwano H, Takahashi T, Mitsudomi T (2004) Mutations of the epidermal growth factor receptor gene in lung cancer: biological and clinical implications. *Cancer Res* 64: 8919–8923

Launonen V (2005) Mutations in the human LKB1/STK11 gene. *Hum Mutat* 26: 291–297

Launonen V, Avizienyte E, Loukola A, Laiho P, Salovaara R, Jarvinen H, Mecklin JP, Oku A, Shimane M, Kim HC, Kim JC, Nezu J, Aaltonen LA (2000) No evidence of Peutz-Jeghers syndrome gene LKB1 involvement in left-sided colorectal carcinomas. *Cancer Res* 60: 546–548

Marchetti A, Martella C, Felicioni L, Barassi F, Salvatore S, Chella A, Camplese PP, Iarussi T, Mucilli F, Mezzetti A, Cuccurullo F, Sacco R, Buttitta F (2005) EGFR mutations in non-small-cell lung cancer: analysis of a large series of cases and development of a rapid and sensitive method for diagnostic screening with potential implications on pharmacologic treatment. *J Clin Oncol* 23: 857–865

Matsumoto S, Iwakawa R, Takahashi K, Kohno T, Nakanishi Y, Matsuno Y, Suzuki K, Nakamoto M, Shimizu E, Minna JD, Yokota J (2007) Prevalence and specificity of LKB1 genetic alterations in lung cancers. *Oncogene* 26: 5911–5918

Naoki K, Chen TH, Richards WG, Sugarbaker DJ, Meyerson M (2002) Missense mutations of the BRAF gene in human lung adenocarcinoma. *Cancer Res* 62: 7001–7003

Ono M, Hirata A, Kometani T, Miyagawa M, Ueda S, Kinoshita H, Fujii T, Kuwano M (2004) Sensitivity to gefitinib (Iressa, ZD1839) in non-small cell lung cancer cell lines correlates with dependence on the epidermal growth factor (EGF) receptor/extracellular signal-regulated kinase 1/2 and EGF receptor/Akt pathway for proliferation. *Mol Cancer Ther* 3: 465–472

Onozato R, Kosaka T, Achiwa H, Kuwano H, Takahashi T, Yatabe Y, Mitsudomi T (2007) LKB1 gene mutations in Japanese lung cancer patients. *Cancer Sci* 98: 174–175

Pham D, Kris MG, Riely GJ, Sarkaria IS, McDonough T, Chuai S, Venkatraman ES, Miller VA, Ladanyi M, Pao W, Wilson RK, Singh B, Rusch VW (2006) Use of cigarette-smoking history to estimate the likelihood of mutations in epidermal growth factor receptor gene exons 19 and 21 in lung adenocarcinomas. *J Clin Oncol* 24: 1700–1704

Sanchez-Cespedes M, Parrella P, Esteller M, Nomoto S, Trink B, Engles JM, Westra WH, Herman JG, Sidransky D (2002) Inactivation of LKB1/STK11 is a common event in adenocarcinomas of the lung. *Cancer Res* 62: 3659–3662

Shaw RJ, Bardeesy N, Manning BD, Lopez L, Kosmatka M, DePinho RA, Cantley LC (2004) The LKB1 tumor suppressor negatively regulates mTOR signaling. *Cancer Cell* 6: 91–99

Tiainen M, Ylikorkala A, Makela TP (1999) Growth suppression by Lkb1 is mediated by a G(1) cell cycle arrest. *Proc Natl Acad Sci USA* 96: 9248–9251

Tracy S, Mukohara T, Hansen M, Meyerson M, Johnson BE, Janne PA (2004) Gefitinib induces apoptosis in the EGFRL858R non-small-cell lung cancer cell line H3255. *Cancer Res* 64: 7241–7244

Volikos E, Robinson J, Aittomaki K, Mecklin JP, Jarvinen H, Westerman AM, de Rooij FW, Vogel T, Moeslein G, Launonen V, Tomlinson IP, Silver AR, Aaltonen LA (2006) LKB1 exonic and whole gene deletions are a common cause of Peutz-Jeghers syndrome. *J Med Genet* 43: e18

N-Glycan fucosylation of epidermal growth factor receptor modulates receptor activity and sensitivity to epidermal growth factor receptor tyrosine kinase inhibitor

Kazuko Matsumoto,[1,3] Hideyuki Yokote,[1] Tokuzo Arao,[1] Mari Maegawa,[1] Kaoru Tanaka,[1] Yoshihiko Fujita,[1] Chikako Shimizu,[2] Toshiaki Hanafusa,[3] Yasuhiro Fujiwara[2] and Kazuto Nishio[1,4]

[1]Department of Genome Biology, Kinki University School of Medicine, 377-2 Ohno-Higashi, Osaka-Sayama, Osaka; [2]Medical Oncology, National Cancer Center Hospital, Tokyo; [3]First Department of Internal Medicine, Osaka Medical College, Osaka, Japan

The glycosylation of cell surface proteins is important for cancer biology processes such as cellular proliferation or metastasis. α1,6-Fucosyltransferase (FUT8) transfers a fucose residue to n-linked oligosaccharides on glycoproteins. Herein, we study the effect of fucosylation on epidermal growth factor receptor (EGFR) activity and sensitivity to an EGFR-specific tyrosine kinase inhibitor (EGFR-TKI). The increased fucosylation of EGFR significantly promoted EGF-mediated cellular growth, and the decreased fucosylation by stable FUT8 knockdown weakened the growth response in HEK293 cells. The overexpression of FUT8 cells were more sensitive than the control cells to the EGFR-TKI gefitinib, and FUT8 knockdown decreased the sensitivity to gefitinib. Finally, to examine the effects in a human cancer cell line, we constructed stable FUT8 knockdown A549 cells, and found that these cells also decreased EGF-mediated cellular growth and were less sensitive than the control cells to gefitinib. In conclusion, we demonstrated that the modification of EGFR fucosylation affected EGF-mediated cellular growth and sensitivity to gefitinib. Our results provide a novel insight into how the glycosylation status of a receptor may affect the sensitivity of the cell to molecular target agents.
(Cancer Sci 2008; 99: 1611–1617)

The glycosylation of cell surface proteins and lipids is modified during the course of differentiation, growth and aging, and various glycoprotein structures are important for biological functions.[1] Proteins and lipids are modified with n-linked oligosaccharides in the endoplasmic reticulum and Golgi apparatus. n-Linked oligosaccharides contribute to the folding and stability of glycoproteins.[2] Various glycosyltransferases have been cloned and are known to be involved in the formation of n-linked oligosaccharides.[3,4] Accumulating data has demonstrated that the modification of glycoforms can even change the phenotype of cells.[5]

Regarding the relationship between malignancy and n-linked oligosaccharides, glycoproteins on the cell surface are known to be altered in both quantity and quality during cancerous transformation.[6] Genes are known to determine the specific structures of oligosaccharides during regulated biological processes involved in cancer, such as metastasis.[7] For example, the knockout of n-acetylglucosaminyltransferase V (GnT-V) has been reported to decrease metastasis in mice, indicating that GnT-V is deeply involved in cancer metastasis.[8]

Epidermal growth factor receptor (EGFR) is frequently expressed or highly expressed in lung cancer, ovarian cancer and many other solid tumors,[9–12] and a high expression level in tumor cells is closely related to a poor prognosis.[13,14] Therefore, EGFR is considered an important therapeutic target for the treatment of solid tumors. Tyrosine kinase inhibitors (TKI) that target EGFR, like gefitinib (IRESSA, ZD1839)[15–17] and erlotinib (Tarceva),[18] and the anti-EGFR antibody cetuximab (IMC-C225),[19] have been reported to exhibit potential antitumor effects in some solid tumors. Dramatic responses to gefitinib have been observed in non-small cell lung cancer (NSCLC) patients harboring activating mutations in the EGFR gene involving an exon 19 deletion or an L858R point mutation in exon 21.[20,21] However, the sensitivity of a cell to EGFR-TKI cannot be completely defined by these mutations because tumor response and disease stabilization with gefitinib have also been reported in some NSCLC patients with wild-type EGFR.[22,23] We have searched for predictive biomarkers that determine sensitivity to molecular targeted agents, including gefitinib.[24,25] Of additional interest, EGFR contains 11 potential n-glycosylation sites in its extracellular domain.[26] α1,6-Fucosyltransferase (FUT8) catalyzes the transfer of a fucose group to the innermost n-acetylglucosamine residue of complex n-glycans via α1,6-linkage in mammals. Wang et al. clearly demonstrated that the fucosylation of EGFR catalyzed by FUT8 regulates its receptor activity and signaling in murine cells.[27] However, whether receptor fucosylation affects the sensitivity of human cells to molecular target agents remains uncertain.

Accordingly, we studied the relationship between the fucosylation status of EGFR and sensitivity to gefitinib in HEK293 and a human NSCLC cell, A549.

Materials and Methods

Reagents. Gefitinib (IRESSA, ZD1839) was provided by AstraZeneca (Cheshire, UK).

Expression constructs and viral production. A full-length cDNA of FUT8, originating from a NSCLC cell line (A549),[28] was amplified using a reverse transcriptase polymerase chain reaction (RT-PCR). A High Fidelity RNA PCR Kit (TaKaRa, Otsu, Japan) was used for the RT-PCR, and the following primer set was synthesized: forward, GGA AGT GAG TTG AAA ATC TGA AA; reverse, ACT GAG TTT GGT CGT TTA TCT CT. The PCR products were amplified again using Pyrobest DNA polymerase (TaKaRa) and the following primer set: forward, GCG CTA GCA ATG CGG CCA TGG ACT GGT TC; reverse, CGT GGT ACC TTT CTC AGC CTC AGG ATA TGT. After confirming the sequence, FUT8 cDNA was transferred to

pcDNA3.1 (Invitrogen, Carlsbad, CA, USA) with a FLAG-tag at its C-terminus. *EGFR* cDNA with a myc-tag in pcDNA3.1 and FUT8 cDNA with a FLAG-tag were cut out and transferred into a pQCLIN retroviral vector (BD Biosciences Clontech, San Diego, CA, USA) together with enhanced green fluorescent protein (EGFP) followed by the internal ribosome entry site sequence (IRES) to monitor the expression of the inserts indirectly. A pVSV-G vector (Clontech, Palo Alt, CA, USA) for the constitution of the viral envelope, pGP vector (TAKARA Bio) and the pQCXIX constructs were co-transfected into the HEK293 cells using FuGene6 transfection reagent (Roche Diagnostics, Basel, Switzerland). Briefly, 80% confluent cells cultured in a 10-cm dish were transfected with 2 μg pVSV-G plus 6 μg pQCXIX vectors. Forty-eight hours after transfection, the culture medium was collected and the viral particles were concentrated by centrifugation at 15 000g for 3 h at 4°C. The viral pellet was then resuspended in fresh RPMI-1640 medium. The titer of the viral vector was calculated by counting the EGFP-positive cells that were infected by serial dilutions of a virus-containing medium and then determining the multiplicity of infection (MOI).

FUT8 knockdown by shRNA. We constructed a retroviral vector that stably expressed short hairpin RNA (shRNA) targeting human FUT8. The DNA sequences were designed as follows: forward, GAT CCG TCT CAG AAT TGG CGC TAT GCT GTG AAG CCA CAG ATG GGC ATA GCG CCA ATT CTG AGA CTT TTT TG; reverse, AAT TCA AAA AAG TCT CAG AAT TGG CGC TAT GCC CAT CTG TGG CTT CAC AGC ATA GCG CCA ATT CTG AGA CG. These oligonucleotides were annealed and inserted into an RNAi-Ready pSIREN-RetroQ-ZsGreen vector (Clontech). The viral particles were produced as described in the viral production section.

Cell culture and transfection. HEK293 (a human embryonic kidney cell line) was maintained in Dulbecco's modified Eagle's medium (DMEM) medium and A549 (an NSCLC cell line) was maintained in RPMI-1640 medium supplemented with 10% fetal bovine serum (FBS). HEK293/EGFR cells were transfected with retrovirus containing FUT8 gene or shRNA for FUT8 (shFUT8) or shRNA control construct and designed as 293/EGFR/FUT8, 293/EGFR/shFUT8 and 293/EGFR/control, respectively. A549 cells were transfected with either shFUT8 or shRNA control and designed as A549/shFUT8 and A549/control, respectively.

α1,6-Fucosyltransferase activity assay. Cells were lysed with a lysis buffer containing 1% Triton X, 20 mM Tris-HCl (pH 8.0) and 50 mM NaCl. The fluorescent substrate (GnGn-bi-Asn-PABA; Fig. 1a) was purchased from Peptide Institute (Osaka, Japan). The standard mixture for measuring FUT8 activity contained 50 μM substrate, 200 mM MES (pH 7.0), 1% Triton X, 500 μM GDP-Fucose and the cell lysate in a final volume of 50 μL. The reaction mixture was incubated at 37°C for 6 h, and the reaction was stopped by heating at 100°C for 1 min. The sample was then centrifuged at 15 000g for 10 min and the supernatant (10 μL) was used for analysis. The product was separated using high-performance liquid chromatography (HPLC) with a TSK-gel ODS-80TM column (4.6 mm × 150 mm). Elution was performed at 55°C with a 20 mM acetate buffer, pH 4.0, containing 0.1% butanol. The fluorescence of the column elute was detected using a fluorescence photometer (Hitachi Fluorescence Spectrophotometer 650–10LC). The excitation and emission wavelengths were observed at 320 and 400 nm, respectively.[29]

Immunoprecipitation and immunoblotting. A549 cells were lysed with a lysis buffer containing 1% Triton X, 20 mM Tris-HCl (pH 7.0), 5 mM ethylenediaminetetraacetic acid (EDTA), 50 mM NaCl, 10 mM Na pyrophosphate, 50 mM NaF, 1 mM Na or-thovanadate, and a Complete Mini protease inhibitor mix (Roche Diagnostics). The cell lysate (1 mg) was immunoprecipitated by incubation with anti-EGFR antibody (Upstate Biotechnology, Lake Placid, NY, USA) overnight, followed by further incubation

with protein-G agarose (Santa Cruz Biotechnology, Santa Cruz, CA, USA) for 1 h and washed with lysis buffer three times. Whole cell lysates and immunoprecipitated samples were separated using sodium dodecylsulfate polyacrylamide gel electrophoresis (SDS-PAGE) and blotted on a polyvinylidene fluoride (PVDF) membrane. The membranes were blocked with 3% bovine serum albumin (BSA) in Tris-buffered saline with 0.05% Tween-20 (TBST) and then probed with monoclonal anti-EGFR antibody (Upstate Biotechnology), monoclonal phospho-tyrosine antibody, p44/42 MAP kinase antibody or phospho-p44/42 MAP kinase antibody (Cell Signaling, Beverly, MA, USA), followed by incubation with a monoclonal or polyclonal HRP-conjugated secondary antibody (Cell Signaling). An enhanced chemiluminescence detection system (GE Healthcare, Buckinghamshire, UK) was then used for visualization. Images were visualized by LAS-3000 (Fujifilm, Tokyo, Japan) and the data were quantified by automated densitometry using Multigauge ver. 3.0 (Fujifilm).

Lectin blotting. Whole cell lysates and immunoprecipitated samples were separated using SDS-PAGE and blotted on a PVDF membrane. The membrane was blocked with 5% BSA in TBST for 1 h at room temperature. The membrane was probed with biotinylated aleuria aurantia lectin (AAL, Seikagaku, Tokyo, Japan) for 1 h at room temperature, washed, and treated using the Vectastain ABC kit (Vector Laboratories, Burlingame, CA, USA) as a second antibody.

Cell proliferation assay. To evaluate the growth response to EGF stimulation, we used the tetrazolium dye (3,4,5-dimethyl-2H-tetrazolium bromide, MTT) assay. The cells were seeded at a density of 0.5–1.5 × 10³ cells/well in 96-well plates under a serum-reduced condition (HEK293 cells, 4% FBS; A549 cells, 2% FBS). Twenty-four hours later, the cells were stimulated with EGF (R&D Systems, Minneapolis, MN, USA) at 20 ng/mL. After 48–72 h of incubation at 37°C, the MTT solution was added to each well and the plates were incubated for 3 h at 37°C. After centrifuging the plates at 400g for 5 min, the medium was discarded from each well, and 200 μL of dimethylsulfoxide was added to each well. The optical density was measured at 570 nm. For the growth curve experiments, the cells were seeded at a density of 2 × 10³ cells/well in 96-well plates in the presence of 10% FBS or under the serum-reduced condition in the presence of 20 ng/mL of EGF. Cell proliferation was estimated by measuring the absorbance at 570 nm at 24 h intervals up to 72 h.

Growth inhibitory assay. To evaluate the growth inhibition in the presence of various concentrations of gefitinib, we used the MTT assay. The cells were seeded at a density of 1.5 or 2 × 10³ cells/well in 96-well plates in the presence of 10% FBS or under the serum-reduced condition in the presence of 20 ng/mL of EGF. Twenty-four hours later, gefitinib was added and the incubation was continued further for 72 h at 37°C. The assay was conducted in triplicate.

Soft agar assay for colony formation. To confirm the data obtained from the growth inhibitory assay, we performed colony assays of A549 cells. Five hundred cells in 0.35% agar in DMEM containing 10% FBS and each concentration of EGF or gefitinib were seeded onto 6-well plates on an underlayer of 0.5% agar containing DMEM. The plates were incubated at 37°C for 14 days, and then the colonies were stained by crystal violet and counted under a microscope. The colony assay was performed in triplicate.

Statistical analysis. All statistical calculations were performed using a Student's t-test by StatView ver. 5 software (SAS Institute, Cary, NC, USA). $P < 0.05$ was considered significant.

Result

Establishment of FUT8 overexpression and knockdown cells. To examine whether an increase or decrease in the fucosylation of

365

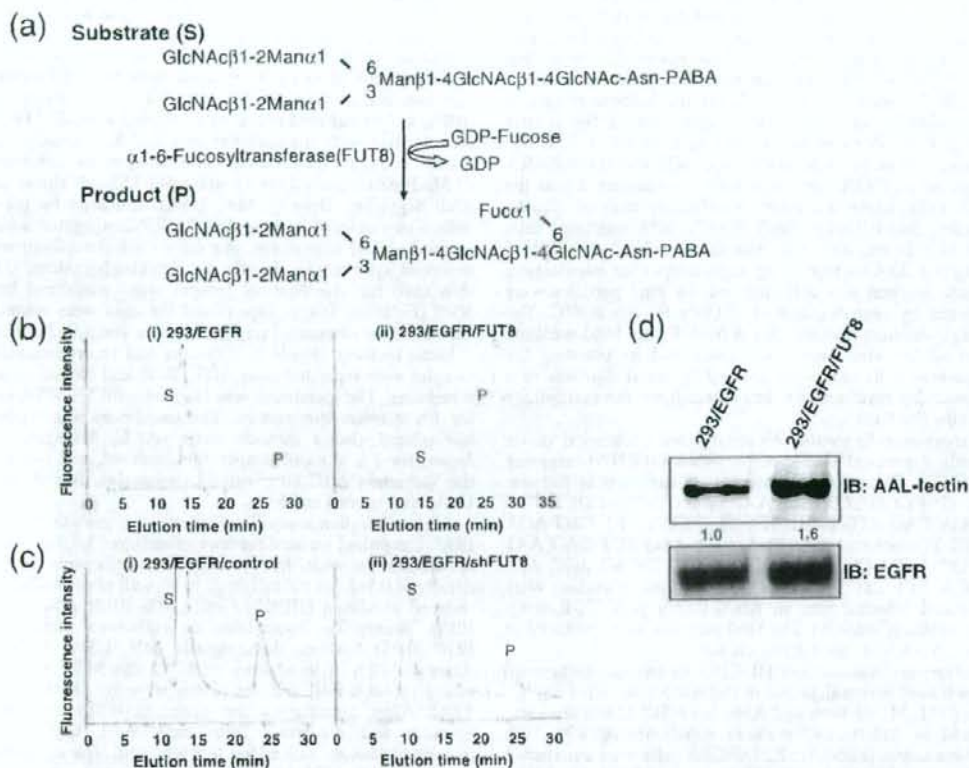**Fig. 1.** α1,6-Fucosyltransferase (FUT8) enzyme activity of HEK293 cells. (a) Schema of FUT8 reaction pathway. Asn, asparagine; Fuc, Fucose; Man, mannose; PABA, 4-(2-pyridylamino) butylamine. (b) Analysis of FUT8 activity in cells overexpressing FUT8. FUT8 activity was measured using high-performance liquid chromatography. (i) 293/EGFR; (ii) 293/EGFR/FUT8. P, product; S, substrate. (c) Analysis of FUT8 activity in FUT8 knockdown cells. (i) 293/EGFR/control; (ii) 293/EGFR/shFUT8. (d) Effect of FUT8 overexpression on epidermal growth factor receptor (EGFR) fucosylation. The cell lysate from 293/EGFR or 293/EGFR/FUT8 cells was subjected to sodium dodecylsulfate polyacrylamide gel electrophoresis followed by lectin blotting using biotinylated *Aleuria aurantia* lectin (AAL). IB, immunoblot.

EGFR affected EGF-mediated cellular growth and sensitivity to gefitinib, we transfected EGFR and FUT8 retrovirally. We also constructed 293/EGFR/shFUT8 cells by the stable knockdown of intrinsic FUT8. FUT8 enzyme activity was measured by reverse-phase HPLC using a fluorescent substrate (GnGn-bi-Asn-PABA; Fig. 1a). FUT8 activity was 25-times higher in 293/EGFR/FUT8 cells than in 293/EGFR (44.1 U/L and 1.8 U/L, respectively; Fig. 1b). On the other hand, the activity in 293/EGFR/shFUT8 cells was 43% of that in 293/EGFR/control cells (Fig. 1c). We next compared fucosylated EGFR between 293/EGFR and 293/EGFR/FUT8 cells using lectin blotting with *Aleuria aurantia* lectin, which recognizes core fucosylation on *n*-glycans. The fucosylation of EGFR was increased in 293/EGFR/FUT8 cells, compared with that in 293/EGFR cells (Fig. 1d). These findings indicated that the overexpression or knockdown of FUT8 was functional and FUT8 regulated the fucosylation of EGFR, as expected.

EGFR fucosylation regulates EGF-mediated cellular growth in HEK293 and A549 cells. We next examined whether EGFR fucosylation affected the cellular growth in response to EGF ligand stimulation. Overexpression of FUT8 was associated with a significant increase, by approximately 20%, of the cellular growth in response to EGF stimulation ($P < 0.05$; Fig. 2a). In

growth curve experiments, the proliferative activity of 293/EGFR/FUT8 cells was slightly increased as compared with that of 293/EGFR cells under normal conditions of culture in the presence of 10% FBS (Fig. 2b). The doubling times of 293/EGFR/FUT8 and 293/EGFR cells were 27.5 and 28.5 h, respectively. However, remarkable increase of the proliferative activity of 293/EGFR/FUT8 cells was observed as compared with that of 293/EGFR cells in the presence of EGF stimulation ($P < 0.05$; Fig. 2c); the doubling times under this condition were 23.9 and 25.4 h, respectively. Next, FUT8 knockdown significantly decreased, by approximately 20%, the cellular growth in response to EGF stimulation ($P < 0.05$; Fig. 2d). In growth curve experiments, there was no difference in the proliferative activity between 293/EGFR/shFUT8 cells and 293/EGFR/control cells under normal conditions of culture (Fig. 2e), but significant decrease of the proliferative activity of 293/EGFR/shFUT8 cells was found as compared with that of the 293/EGFR/control cells in the presence of EGF stimulation ($P < 0.05$; Fig. 2f); the doubling times of the 293/EGFR/shFUT8 and 293/EGFR/control cells under this condition were 28.8 and 27.3 h, respectively. These findings suggest that the level of EGFR fucosylation regulated the cellular growth in response to EGF. To study whether the same phenomenon
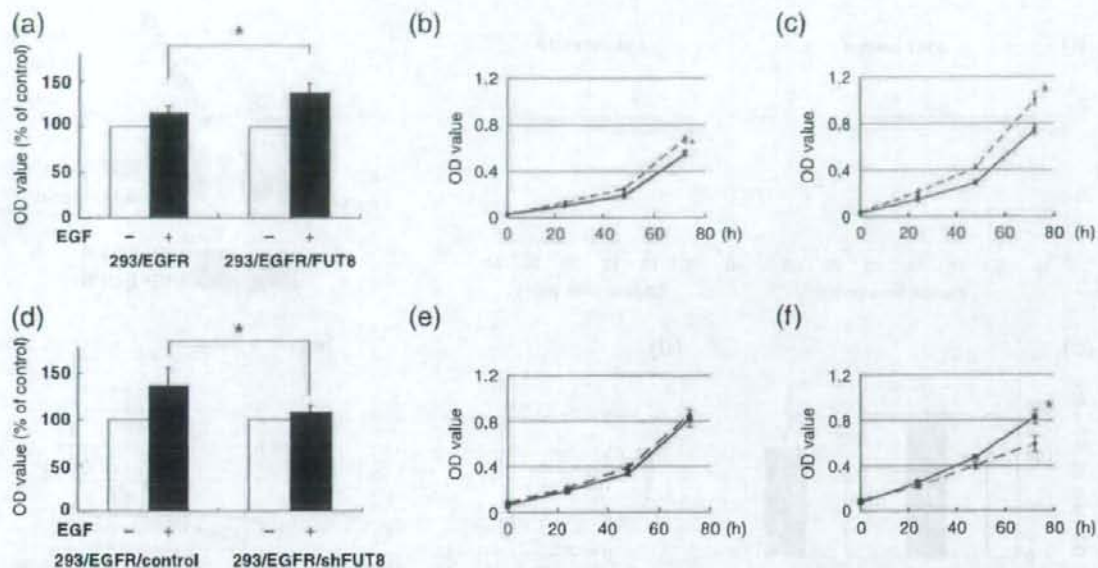
Fig. 2. Cellular growth response to epidermal growth factor (EGF) stimulation in HEK293 cells. (a) The 293/EGFR and 293/EGFR/FUT8 cells were seeded (1.5×10^3 cells/well) in 96-well plates under a serum-reduced condition and stimulated with 20 ng/mL of EGF and further incubated for 48 h at 37°C. (□), EGF (−); (■), EGF (+). (b) Growth curve experiments in the 293/EGFR (solid line) and 293/EGFR/FUT8 (dotted line) cells. The cells were cultured under a 10% fetal bovine serum (FBS) condition. (c) The 293/EGFR (solid line) and 293/EGFR/FUT8 (dotted line) cells were cultured under the presence of 20 ng/mL of EGF to a serum-reduced condition. (d) The 293/EGFR/control and 293/EGFR/shFUT8 cells were seeded (1.5×10^3 cells/well) in 96-well plates under a serum-reduced condition and stimulated with 20 ng/mL of EGF and incubated for 72 h at 37°C. (□), EGF (−); (■), EGF (+). (e) Growth curve experiments in the 293/EGFR/control (solid line) and 293/EGFR/shFUT8 (dotted line) cells. The cells were cultured under a 10% FBS condition. (f) The 293/EGFR/control (solid line) and 293/EGFR/shFUT8 (dotted line) cells were cultured under the presence of 20 ng/mL of EGF to a serum-reduced condition. OD value, 570 nm. *$P < 0.05$; scale lines, standard deviation (SD).

occurs in human cancer cells, we constructed A549/shFUT8, in which FUT8 was stably knocked down, and examined the relationship between the fucosylation level of EGFR and the response to EGF ligand stimulation. No FUT8 catalytic activity was detected by FUT8 knockdown in the A549 cells (Fig. 3a). A lectin blot analysis demonstrated that the fucosylation of EGFR was decreased in A549/shFUT8 cells, while the expression level of EGFR was similar in the control cells (Fig. 3b). We examined whether this reduction in EGFR fucosylation affected the EGF-mediated growth response. We found that A549/shFUT8 cells had significantly decreased EGF-mediated cellular growth by approximately 20%, compared with control cells ($P < 0.05$; Fig. 3c) by the MTT assay. In the growth curve experiments, a slight decrease of the proliferative activity of the A549/shFUT8 cells was observed as compared with that of the A549/control cells under normal conditions of culture in the presence of 10% FBS (Fig. 3d); the doubling times of the A549/shFUT8 and A549/control cells were 23.1 and 22.7 h, respectively. However, the A549/shFUT8 cells showed marked decrease of proliferative activity as compared with A549/control cells in the presence of EGF stimulation ($P < 0.05$, Fig. 3e); the doubling times of the A549/shFUT8 and A549/control cells were 22.2 and 20.8 h, respectively. These results suggest that the level of EGFR fucosylation regulated the cellular growth in response to EGF even in human cancer cells.

Modification of EGFR fucosylation affects cell sensitivity to gefitinib. We then examined whether an increase or decrease in EGFR fucosylation affected the sensitivity of HEK293 cells to gefitinib. Overexpression of FUT8 significantly enhanced cellular sensitivity to gefitinib as compared with that of the control cells in the presence of EGF under a serum-reduced condition; the IC_{50} values of the drug for these cells were 3.5 ± 0.1 and 5.6 ± 0.3, respectively ($P < 0.05$; Fig. 4a). However, no significant difference in the IC_{50} values of the drug was noted between the two types of cells under normal culture conditions in the presence of 10% FBS (Fig. 4b). In addition, FUT8 knockdown significantly decreased the cellular sensitivity to gefitinib as compared with that of the control cells in the presence of EGF under the serum-reduced condition; the IC_{50} values of the drug for these cells were 7.3 ± 0.4 and 4.4 ± 1.0, respectively ($P < 0.05$; Fig. 4c). On the other hand, no significant difference in the IC_{50} values of the drug were noted among the cells when they were cultured under normal conditions (Fig. 4d). These results suggest that EGFR fucosylation modulates the cellular sensitivity to gefitinib.

We also examined the sensitivity of A549 cells to gefitinib. FUT8 knockdown significantly decreased the sensitivity of the A549 cells to gefitinib in the presence of 20 ng/mL of EGF under the serum-reduced condition; the IC_{50} values of the A549/shFUT8 and A549/control cells were 3.1 ± 0.3 and 1.3 ± 0.2, respectively ($P < 0.05$; Fig. 5a). However, no significant difference in the IC_{50} values were noted among the cells when they were cultured under normal conditions, similar to the observations for HEK293 cells (Fig. 5b). These results suggest that the EGFR fucosylation level affected the sensitivity of human cancer cells to gefitinib. To confirm the data obtained from the growth inhibitory assay, we performed colony assays with the A549 cells. Colony formation of A549/control, but not of the A549/shFUT8 cells, was significantly inhibited by 1 μM gefitinib ($P < 0.05$; Fig. 5c).
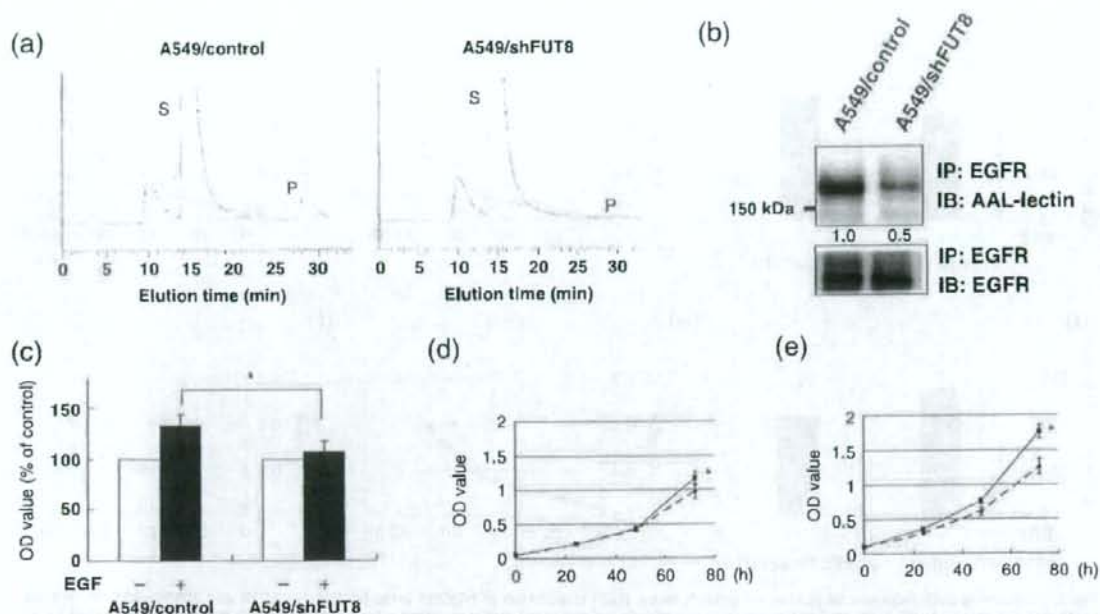
Fig. 3. α1,6-Fucosyltransferase (FUT8) knockdown weakened growth response to epidermal growth factor (EGF) stimulation in A549 cells. (a) FUT8 activity was analyzed using high-performance liquid chromatography. P, product; S, substrate. (b) Effect of FUT8 knockdown on EGF receptor (EGFR) fucosylation in A549 cells. The cell lysate was immunoprecipitated using anti-EGFR antibody, and the sample was separated using sodium dodecylsulfate polyacrylamide gel electrophoresis followed by blotting biotinylated *Aleuria aurantia* lectin (AAL) or monoclonal anti-EGFR antibody. IB, immunoblot; IP, immunoprecipitate. (c) The cells were seeded (0.5 × 10³ cells/well) in 96-well plates under a serum-reduced condition. Twenty-four hours later, the cells were stimulated with 20 ng/mL of EGF and further incubated for 48 h. (□, EGF (–); (■), EGF (+). (d) Growth curve experiments in the A549/control (solid line) and A549/shFUT8 (dotted line) cells. The cells were cultured under a 10% fetal bovine serum condition. (e) The A549/control (solid line) and A549/shFUT8 (dotted line) cells were cultured under the presence of 20 ng/mL of EGF to a serum-reduced condition. OD value, 570 nm. *$P < 0.05$; scale lines, standard deviation.

Fucosylation status of EGFR regulates EGFR signaling. We examined the effect of FUT8 knockdown on the phosphorylation levels of EGFR and the EGFR-mediated intracellular signaling pathway in A549 cells. FUT8 knockdown decreased the phosphorylation levels of EGFR in the presence of EGF stimulation (Fig. 5d). FUT8 knockdown also decreased the EGF-mediated phosphorylation of mitogen-activated protein kinase in the presence of 0.2 and 2 ng/mL of EGF (Fig. 5e). These results suggest that low EGFR fucosylation levels decrease the EGFR-mediated intracellular signaling pathway's response to EGF stimulation.

Discussion

The purpose of this study was to investigate whether the modification of EGFR fucosylation affected EGF-mediated cellular growth and cell sensitivity to gefitinib. We found that the increase in EGFR fucosylation resulting from FUT8 overexpression enhanced the response to EGF stimulation and the sensitivity of the cells to gefitinib. A decrease in EGFR fucosylation resulting from FUT8 knockdown weakened the EGF-mediated cellular growth response and cell sensitivity.

Two possible mechanisms may explain how EGFR fucosylation affects the EGF-mediated growth response. First, the binding affinity of EGFR to the EGF ligand might be affected by the modified fucosylation of the receptor. n-Acetylglucosaminyl-transferase III (GnT III) is known to catalyze the addition of n-acetylglucosamine in β1-4 linkage to the β-linked mannose of the trimannosyl core of n-linked oligosaccharides to produce a

bisecting GlcNac residue. Rebbaa et al. reported that the overexpression of GnT III in glioma cells modifies the glycosylation of its receptor, resulting in a decrease in EGF binding and EGFR autophosphorylation;[30] this finding suggests that the carbohydrate structure at the extracellular domain of EGFR affects the binding affinity with its ligand and the receptor activity. This evidence supports this first possible mechanism. Another possibility is that the ability of the receptor to form dimers might be affected by the glycosylation of the receptor. Tsuda et al. reported that a specific n-glycosylation mutant of domain III of EGFR leads to ligand-independent dimerization and phosphorylation, resulting in the spontaneous activation of the receptor.[31] These findings indicate that n-linked oligosaccharides in extracellular domain III of EGFR play a crucial role in receptor dimerization, independent of ligand binding. The type III EGFR (EGFRvIII), which lacks exons 2–7 in the extracellular domain, is constitutively phosphorylated independently of EGF-ligand stimulation. Fernandes et al. demonstrated that the receptor–receptor self association is highly dependent on a conformation induced by n-linked glycosylation, suggesting that n-linked oligosaccharides play an important role in this autodimerization.[32]

Regarding fucosylation, Wang et al. reported that EGF decreased EGF binding to EGFR in Fut8 knockout mice, resulting in a higher responsiveness of the receptor to its ligand.[27] Many studies have reported that the *mutant* EGFR (i.e. 15-base deletion or L858R) signaling is constitutively active without ligand condition. Thus, we speculated that wild-type EGFR
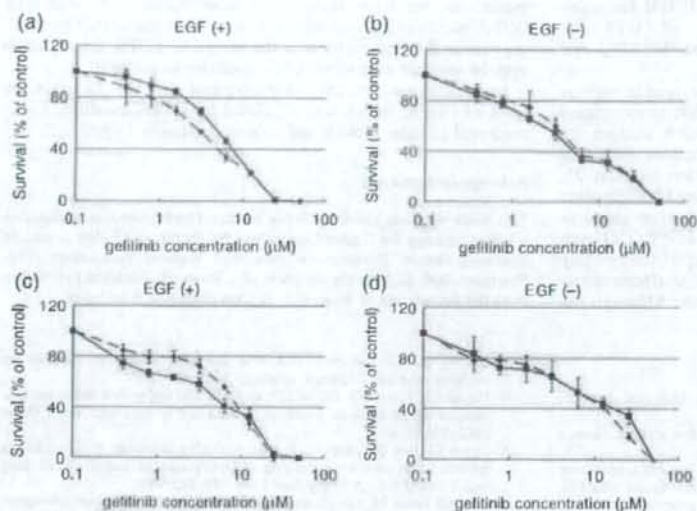
368

Fig. 4. Sensitivity of HEK293 cells to gefitinib. The cells were seeded at a density of 2×10^3 cells/well in 96-well plates. Twenty-four hours later, the cells were exposed to gefitinib and were then incubated for 72 h at 37°C. The cell growth was quantitated using an 3,4,5-dimethyl-2H-tetrazolium bromide (MTT) assay. (a) 293/EGFR (solid line) and 293/EGFR/FUT8 (dotted line) were cultured under the presence of 20 ng/mL of EGF to a serum-reduced condition. (b) 293/EGFR (solid line) and 293/EGFR/FUT8 (dotted line) were cultured under a 10% fetal bovine serum (FBS) condition. (c) 293/EGFR/control cells (solid line) and 293/EGFR/shFUT8 cells (dotted line) were cultured under the presence of 20 ng/mL of EGF to a serum-reduced condition. (d) 293/EGFR/control cells (solid line) and 293/EGFR/shFUT8 cells (dotted line) were cultured under a 10% FBS condition. Scale lines, standard deviation.
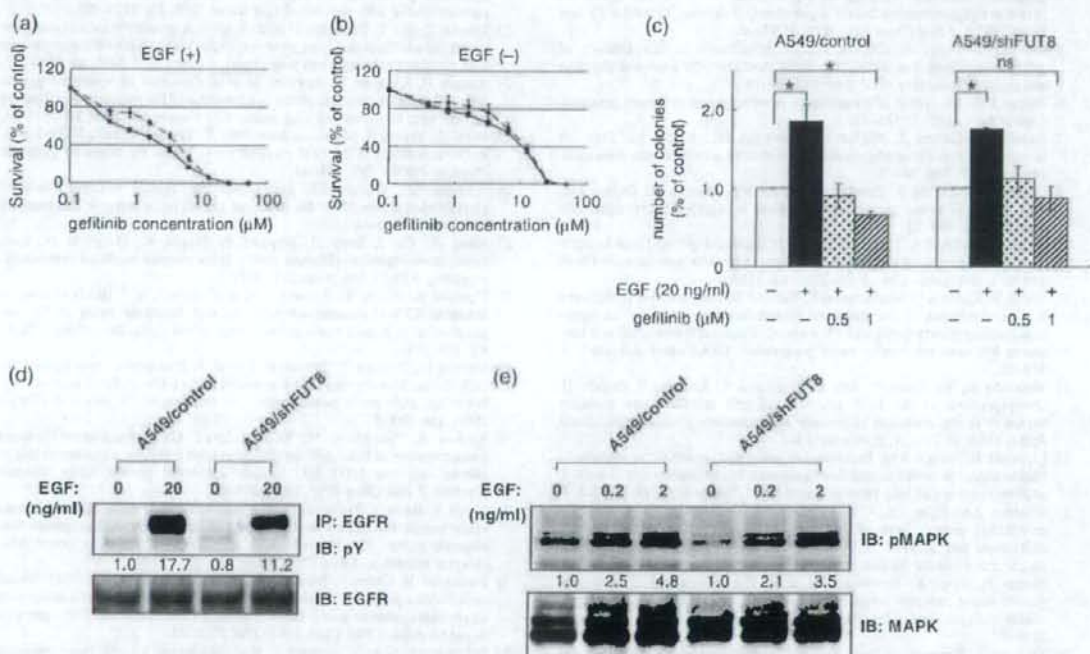

Fig. 5. α1,6-Fucosyltransferase (FUT8) knockdown decreased the sensitivity of A549 cells to gefitinib, epidermal growth factor receptor (EGFR) phosphorylation and EGFR-mediated intracellular signaling. (a) A549/control cells (solid line) and A549/shFUT8 cells (dotted line) were seeded at a density of 1.5×10^3 cells/well in 96-well plates. Twenty-four hours later, the cells were exposed to gefitinib and were then incubated for 72 h at 37°C. The cells were cultured under the presence of 20 ng/mL of EGF to a serum-reduced condition. (b) A549/control cells (solid line) and A549/shFUT8 cells (dotted line) were cultured under a 10% fetal bovine serum condition. Scale lines, standard deviation (SD). (c) Colony assay in A549/control cells and A549/shFUT8 cells. The cells were cultured for 14 days under the presence or absence of EGF or gefitinib. *$P < 0.05$; scale lines, SD. (d) A549 cells were cultured under a serum-free condition for 6 h, and the cells were stimulated with 20 ng/mL of EGF for 10 min. The cell lysate was immunoprecipitated using anti-EGFR antibody and immunoblotted using antiphospho-tyrosine antibody (pY). (e) A549 cells were stimulated with 0.2 ng/mL or 2 ng/mL EGF for 10 min. The cell lysate was separated using sodium dodecylsulfate polyacrylamide gel electrophoresis and then immunoblotted using antiphospho p44/42 mitogen-activated protein kinase (pMAPK) antibody and antip44/42 MAPK (MAPK) antibody. IB, immunoblot; IP, immunoprecipitate.

might be suitable for a study of the effects of fucosylation. Our results also demonstrate that modifications of EGFR fucosylation through the overexpression or knockdown of FUT8 alter EGF-mediated cellular growth responses in both HEK293 and A549 cells.

Epidermal growth factor receptor is overexpressed in various human tumors, and the overexpression of EGFR is associated with a poor prognosis.[33] Many researchers have studied the biological and clinical significance of *EGFR* mutations, including exon 19 deletions and the L858R point mutation in exon 21, which behave like constitutively-active receptors.[34-36] Patients with constitutively-active mutants of *EGFR* are more sensitive to gefitinib. However, some patients respond to EGFR-TKI even though they do not carry such *EGFR* mutations;[22,23] suggesting the presence of one or more undefined factors that affects sensitivity to gefitinib in addition to *EGFR* mutations. Although the

impact on sensitivity to gefitinib is smaller than that of EGFR mutations, we have shown that modifications in wild-type EGFR fucosylation also affect sensitivity to gefitinib. Our findings raise the possibility that the status of EGFR fucosylation may be another determinant of sensitivity to gefitinib.

In conclusion, we have demonstrated that the fucosylation level of EGFR, which was regulated by FUT8, modifies EGF-mediated cellular growth and affects sensitivity to gefitinib.

Acknowledgments

References

1 Hakomori Si SI. Inaugural Article: The glycosynapse. *Proc Natl Acad Sci USA* 2002; **99**: 225–32.
2 Helenius A, Aebi M. Intracellular functions of N-linked glycans. *Science* 2001; **291**: 2364–9.
3 Sato T, Furukawa K, Bakker H, Van den Eijnden DH, Van Die I. Molecular cloning of a human cDNA encoding beta-1,4-galactosyltransferase with 37% identity to mammalian UDP-Gal: GlcNAc beta-1,4-galactosyltransferase. *Proc Natl Acad Sci USA* 1998; **95**: 472–7.
4 Almeida R, Amado M, David L *et al.* A family of human beta4-galactosyltransferases. Cloning and expression of two novel UDP-galactose: beta-n-acetylglucosamine beta1, 4-galactosyltransferases, beta4Gal-T2 and beta4Gal-T3. *J Biol Chem* 1997; **272**: 31 979–91.
5 Coetzee T, Fujita N, Dupree J *et al.* Myelination in the absence of galactocerebroside and sulfatide: normal structure with abnormal function and regional instability. *Cell* 1996; **86**: 209–19.
6 Dennis JW. Asn-linked oligosaccharide processing and malignant potential. *Cancer Surv* 1988; **7**: 573–95.
7 Dennis JW, Laferte S, Waghorne C, Breitman ML, Kerbel RS. Beta 1-6 branching of Asn-linked oligosaccharides is directly associated with metastasis. *Science* 1987; **236**: 582–5.
8 Granovsky M, Fata J, Pawling J, Muller WJ, Khokha R, Dennis JW. Suppression of tumor growth and metastasis in Mgat5-deficient mice. *Nat Med* 2000; **6**: 306–12.
9 Ang KK, Berkey BA, Tu X *et al.* Impact of epidermal growth factor receptor expression on survival and pattern of relapse in patients with advanced head and neck carcinoma. *Cancer Res* 2002; **62**: 7350–6.
10 Rusch V, Klimstra D, Venkatraman E, Pisters PW, Langenfeld J, Dmitrovsky E. Overexpression of the epidermal growth factor receptor and its ligand transforming growth factor alpha is frequent in resectable non-small cell lung cancer but does not predict tumor progression. *Clin Cancer Res* 1997; **3**: 515–22.
11 Watanabe K, Tachibana O, Sata K, Yonekawa Y, Kleihues P, Ohgaki H. Overexpression of the EGF receptor and p53 mutations are mutually exclusive in the evolution of primary and secondary glioblastomas. *Brain Pathol* 1996; **6**: 217–23; discussion 23–4.
12 Lipponen P, Eskelinen M. Expression of epidermal growth factor receptor in bladder cancer as related to established prognostic factors, oncoprotein (c-erbB-2, p53) expression and long-term prognosis. *Br J Cancer* 1994; **69**: 1120–5.
13 Khorana AA, Ryan CK, Cox C, Eberly S, Sahasrabudhe DM. Vascular endothelial growth factor, CD68, and epidermal growth factor receptor expression and survival in patients with Stage II and Stage III colon carcinoma: a role for the host response in prognosis. *Cancer* 2003; **97**: 960–8.
14 Magne N, Pivot X, Bensadoun RJ *et al.* The relationship of epidermal growth factor receptor levels to the prognosis of unresectable pharyngeal cancer patients treated by chemo-radiotherapy. *Eur J Cancer* 2001; **37**: 2169–77.
15 Koizumi F, Kanzawa F, Ueda Y *et al.* Synergistic interaction between the EGFR tyrosine kinase inhibitor gefitinib ('Iressa') and the DNA topoisomerase I inhibitor CPT-11 (irinotecan) in human colorectal cancer cells. *Int J Cancer* 2004; **108**: 464–72.
16 Naruse I, Ohmori T, Ao Y *et al.* Antitumor activity of the selective epidermal growth factor receptor-tyrosine kinase inhibitor (EGFR-TKI) Iressa (ZD1839) in an EGFR-expressing multidrug-resistant cell line in vitro and in vivo. *Int J Cancer* 2002; **98**: 310–15.
17 Fukuoka M, Yano S, Giaccone G *et al.* Multi-institutional randomized phase II trial of gefitinib for previously treated patients with advanced non-small-cell lung cancer. *J Clin Oncol* 2003; **21**: 2237–46.

18 Sandler A. Clinical experience with the HER1/EGFR tyrosine kinase inhibitor erlotinib. *Oncology (Huntingt)* 2003; **17**: 17–22.
19 Herbst RS, Hong WK. IMC-C225, an anti-epidermal growth factor receptor monoclonal antibody for treatment of head and neck cancer. *Semin Oncol* 2002; **29**: 18–30.
20 Lynch TJ, Bell DW, Sordella R *et al.* Activating mutations in the epidermal growth factor receptor underlying responsiveness of non-small-cell lung cancer to gefitinib. *N Engl J Med* 2004; **350**: 2129–39.
21 Paez JG, Janne PA, Lee JC *et al.* EGFR mutations in lung cancer: correlation with clinical response to gefitinib therapy. *Science* 2004; **304**: 1497–500.
22 Han SW, Kim TY, Hwang PG *et al.* Predictive and prognostic impact of epidermal growth factor receptor mutation in non-small-cell lung cancer patients treated with gefitinib. *J Clin Oncol* 2005; **23**: 2493–501.
23 Takano T, Ohe Y, Sakamoto H *et al.* Epidermal growth factor receptor gene mutations and increased copy numbers predict gefitinib sensitivity in patients with recurrent non-small-cell lung cancer. *J Clin Oncol* 2005; **23**: 6829–37.
24 Kimura H, Kasahara K, Kawaishi M *et al.* Detection of epidermal growth factor receptor mutations in serum as a predictor of the response to gefitinib in patients with non-small-cell lung cancer. *Clin Cancer Res* 2006; **12**: 3915–21.
25 Sakai K, Yokote H, Murakami-Murofushi K, Tamura T, Saijo N, Nishio K. In-frame deletion in the EGF receptor alters kinase inhibition by gefitinib. *Biochem J* 2006; **397**: 537–43.
26 Whitson KB, Whitson SR, Red-Brewer ML *et al.* Functional effects of glycosylation at Asn-579 of the epidermal growth factor receptor. *Biochemistry* 2005; **44**: 14 920–31.
27 Wang X, Gu J, Ihara H, Miyoshi E, Honke K, Taniguchi N. Core fucosylation regulates epidermal growth factor receptor-mediated intracellular signaling. *J Biol Chem* 2006; **281**: 2572–7.
28 Fukuoka K, Nishio K, Fukumoto H *et al.* Ectopic p16 (ink4) expression enhances CPT-11-induced apoptosis through increased delay in S-phase progression in human non-small-cell-lung-cancer cells. *Int J Cancer* 2000; **86**: 197–203.
29 Uozumi N, Teshima T, Yamamoto T *et al.* A fluorescent assay method for GDP-L-Fuc: N-acetyl-beta-D-glucosaminide alpha 1-6fucosyltransferase activity, involving high performance liquid chromatography. *J Biochem (Tokyo)* 1996; **120**: 385–92.
30 Rebbaa A, Yamamoto H, Saito T *et al.* Gene transfection-mediated overexpression of beta1,4-N-acetylglucosamine bisecting oligosaccharides in glioma cell line U373 MG inhibits epidermal growth factor receptor function. *J Biol Chem* 1997; **272**: 9275–9.
31 Tsuda T, Ikeda Y, Taniguchi N. The Asn-420-linked sugar chain in human epidermal growth factor receptor suppresses ligand-independent spontaneous oligomerization. Possible role of a specific sugar chain in controllable receptor activation. *J Biol Chem* 2000; **275**: 21 988–94.
32 Fernandes H, Cohen S, Bishayee S. Glycosylation-induced conformational modification positively regulates receptor–receptor association: a study with an aberrant epidermal growth factor receptor (EGFRvIII/DeltaEGFR) expressed in cancer cells. *J Biol Chem* 2001; **276**: 5375–83.
33 Selvaggi G, Novello S, Torri V *et al.* Epidermal growth factor receptor overexpression correlates with a poor prognosis in completely resected non-small-cell lung cancer. *Ann Oncol* 2004; **15**: 28–32.
34 Tracy S, Mukohara T, Hansen M, Meyerson M, Johnson BE, Janne PA. Gefitinib induces apoptosis in the EGFRL858R non-small-cell lung cancer cell line H3255. *Cancer Res* 2004; **64**: 7241–4.
35 Chen YR, Fu YN, Lin CH *et al.* Distinctive activation patterns in constitutively active and gefitinib-sensitive EGFR mutants. *Oncogene* 2006; **25**: 1205–15.
36 Sordella R, Bell DW, Haber DA, Settleman J. Gefitinib-sensitizing EGFR mutations in lung cancer activate anti-apoptotic pathways. *Science* 2004; **305**: 1163–7.

370

Nonplatinum-based Chemotherapy With Irinotecan Plus Docetaxel for Advanced or Metastatic Olfactory Neuroblastoma

A Retrospective Analysis of 12 Cases

Naomi Kiyota, MD[1]
Makoto Tahara, MD, PhD[1]
Satoshi Fujii, MD, PhD[2]
Mitsuhiko Kawashima, MD[3]
Takashi Ogino, MD[3]
Hironobu Minami, MD[4]
Ryuichi Hayashi, MD[5]
Atsushi Ohtsu, MD[1]

[1] Division of Gastrointestinal Oncology and Digestive Endoscopy, National Cancer Center Hospital East, Kashiwa, Chiba, Japan.

[2] Division of Pathology, National Cancer Center Hospital East, Kashiwa, Chiba, Japan.

[3] Division of Radiation Oncology, National Cancer Center Hospital East, Kashiwa, Chiba, Japan.

[4] Division of Oncology/Hematology, National Cancer Center Hospital East, Kashiwa, Chiba, Japan.

[5] Division of Head and Neck Surgery, National Cancer Center Hospital East, Kashiwa, Chiba, Japan.

BACKGROUND. The efficacy and safety of chemotherapy with irinotecan plus docetaxel were retrospectively evaluated for olfactory neuroblastoma.

METHODS. Twelve patients with histologically proven advanced or metastatic olfactory neuroblastoma were treated with chemotherapy with irinotecan plus docetaxel at the study institution between 2001 and 2005. Of these, 7 patients with locoregional disease and no prior radiotherapy received irinotecan plus docetaxel followed by definitive radiotherapy, 1 with photon radiotherapy and 6 with proton radiotherapy, whereas 3 patients with distant metastases and 2 with locoregional disease who had received prior radiotherapy received irinotecan plus docetaxel only.

RESULTS. The most common toxicities of ≥grade 3 among the 12 patients receiving irinotecan plus docetaxel were leukopenia (33%), neutropenia (50%), febrile neutropenia (8%), and diarrhea (25%), all of which were manageable. Partial response was achieved in 3 patients, giving an overall response rate of 25%. The response rate was higher in patients aged <50 years (3 of 4 patients) compared with those aged >50 years (0 of 8 patients) ($P = .018$). With a median follow-up period of 22.2 months, the median progression-free survival and overall survival were 13.6 months and 36.6 months, respectively. Of the 7 patients with locoregional disease also receiving definitive radiotherapy, the 2-year survival rate was 100% and 6 patients were alive at the time of last follow-up.

CONCLUSIONS. Chemotherapy for olfactory neuroblastoma with irinotecan plus docetaxel is safe and manageable. Patients aged <50 years may be sensitive to chemotherapy. Induction chemotherapy followed by definitive radiotherapy may represent a promising option for patients with locally advanced olfactory neuroblastoma. *Cancer* 2008;112:885–91. © 2008 American Cancer Society.

KEYWORDS: olfactory neuroblastoma, chemotherapy, irinotecan, docetaxel, proton radiotherapy.

Olfactory neuroblastoma (ONB), also known as esthesioneuroblastoma, is a rare tumor arising from the olfactory epithelium of the upper nasal cavity.[1,2] ONB accounts for 3% of all intranasal tumors[3] and its etiology is unknown. Since its first description by Berger and Luc in 1924,[4] approximately 1000 cases have been reported in the literature.[5] The sex distribution is roughly equal.[2,5] Although several authors have demonstrated a bimodal distribution in the age of diagnosis, with peaks in those aged 11 to 20 years and 51 to 60 years,[2,6] others have described a unimodal distribution concentrating in the fifth decade of life.[7]

With regard to treatment, the combination of surgery and radiotherapy is the most frequent approach and offers the highest cure rates,[8-12] but definitive radiotherapy as a nonsurgical treatment is also used.[2,10,12-14] However, despite definitive local treatment, local recurrence and distant metastases are often reported,[6,8,12] with the latter observed in 25% to 50% of cases.[15-19] Chemotherapy is therefore often also implemented in patients with recurrent or metastatic ONB. Experience at several institutions using various chemotherapeutic regimens has suggested that this tumor might be sensitive to chemotherapy,[7,8,18,20-22] but its rarity has prevented any clear determination of the role of chemotherapy or the optimal chemotherapy regimen.

Between 1995 and 2005, our group at the National Cancer Center Hospital East treated 20 patients with either or both advanced or metastatic ONB with chemotherapy. Results with a variety of chemotherapy regimens used before 2001, including platinum-based regimens,[23] were unsatisfactory, leading us to speculate on the possibility of using irinotecan plus docetaxel (ID). In addition, in patients with locoregional disease we adopted proton radiotherapy after induction chemotherapy with ID because of its lower radiotoxicity to adjacent tissues (brain, optic nerve, eyeball, etc).[24]

Investigation of this regimen in 3 ONB patients in a phase 1 study of ID for solid cancer produced a good response in 2.[25] The first, who had previously received platinum-based chemotherapy at our institution, was responsive to ID, with a response duration of approximately 10 months. The second, a chemotherapy-naive patient with locoregional disease, achieved a partial response with ID, and a subsequent complete response (CR) after proton radiotherapy after ID. We therefore decided to treat not only recurrent or metastatic ONB but also locoregional ONB with ID, and since 2001 have treated 12 patients with this regimen. Of these, 7 with locoregional disease and no prior radiotherapy received ID followed by definitive radiotherapy, namely, photon radiotherapy in 1 patient and proton radiotherapy in 6 patients.

In this retrospective analysis, we evaluated the efficacy and toxicity of chemotherapy with ID for ONB and the efficacy of ID followed by definitive radiotherapy for locally advanced ONB. After suggestions from several authors that the pathologic features of ONB might correlate with prognosis and response to chemotherapy,[1,10,18,26-28] we also analyzed the correlation between response and the histologic grading of Hyams.[28]

MATERIALS AND METHODS

We reviewed the clinical records of the 12 patients with ONB treated with ID at the National Cancer Center Hospital East between 2001 and 2005. All 12 had histologically proven ONB and pathologic specimens were available for 10 patients. These were reviewed according to the histologic grading system of Hyams[28], and the correlation between Hyams grade and response to ID was analyzed.

Response to chemotherapy was evaluated using the World Health Organization (WHO) standard response criteria.[29] Chemotherapy-related toxicities were graded by the National Cancer Center Institute Common Toxicity Criteria (version 2). Overall survival time was calculated from the initiation of chemotherapy with ID to the date of death or last follow-up, whichever occurred first. Progression-free survival time was calculated from the initiation of chemotherapy with ID to the documentation of progression or death. Actuarial survival was estimated by the Kaplan-Meier method.[30] Statistical analysis of categoric data was performed using a Fisher exact test. Differences were considered statistically significant at $P < .05$. All analyses were conducted using the statistical analysis software Stat View-J (version 5.0) for Windows (SAS Institute Inc, Cary, NC).

RESULTS
Patient Characteristics

Patient characteristics are summarized in Table 1. The 4 males and 8 females ranged in age from 24 to 73 years, with a median age of 58.5 years. According to the clinical staging system of Kadish and Wang,[1] 2 patients had stage B disease at the time of chemotherapy and 10 had stage C disease. The primary site was determined by either or both computed tomography scanning and magnetic resonance imaging. Intracranial invasion was noted in 5 patients, regional lymph node metastases in 6, and distant metastases in 3. The site of metastases in these 3 patients was the lung and liver; cervical lymph node, lung, and bone; and cervical lymph node and bone in 1 patient each. Of the 12 patients, 9 presented with locoregional disease and 3 initially presented with distant metastases. Of the 9 patients with locoregional disease, 2 had received prior radiotherapy, whereas 7 had not.

Of the 12 patients with histologically proven ONB, specimens for pathologic review were available for 10. Of these, 2 tumors were low grade (Hyams grade I/II) and 8 were high grade (Hyams rade III/IV).

TABLE 1
Patient Characteristics and Treatment Course in Individual Patients

Age, year	Gender	ECOG PS	Kadish stage	ICI	LR/DM	Metastatic site	Prior treatment	Chemotherapy	Response	Subsequent treatment	RT/PRT	Survival, months	Status
65	Woman	1	C	+	DM	L, H	S, RT	ID	PD	Chemotherapy	—	5.7	DWD
24	Woman	0	C	—	DM	LN, L, B	—	ID	PD	Palliative RT	—	6.5	DWD
36	Woman	1	C	+	DM	LN, B	S, chemotherapy, RT	ID	PR	Chemotherapy	—	22.5	DWD
54	Man	0	C	—	LR	LN	S, RT, chemotherapy	ID	NC	—	—	16.1	DWD
59	Woman	1	C	—	LR	LN	S, RT	ID	NC	—	—	29.7	AWD
73	Man	0	C	—	LR	—	S	ID	PD	PRT	CR	14.8	AWD
58	Woman	0	C	+	LR	—	—	ID	NC	PRT	CR	16.1	ANED
48	Woman	0	C	—	LR	LN	—	ID	PR	PRT	CR	19.6	ANED
61	Man	0	B	—	LR	—	—	ID	NC	RT	CR	22.2	ANED
66	Woman	0	B	—	LR	—	—	ID	NC	PRT	PR	36.6	DWD
32	Man	0	C	+	LR	—	—	ID	PR	PRT	CR	53.4	ANED
61	Woman	1	C	+	LR	LN	Chemotherapy	ID	NC	PRT, chemotherapy	PR	63.0	AWD

PS indicates performance status; ICI, intercranial invasion; LR, locoregional; DM: distant metastases; RT, radiotherapy; PRT, proton radiotherapy; ECOG, Eastern Cooperative Oncology Group; +, positive; 1, lung; H, liver; S, surgery; ID, irinotecan plus docetaxel; PD, progressive disease; DWD, dead with disease; —, negative; LN, lymph node; B, bone; PR, partial response; NC, no change; AWD, alive with disease; CR, complete response; ANED, alive with no evidence of disease.

Treatment Results

Treatment results are also listed in Table 1. All 12 patients received chemotherapy with ID, given as 3 weekly administrations of both irinotecan at a dose of 50 to 60 mg/m^2 on Day 1 and docetaxel at a dose of 30 to 35 mg/m^2 on Day 1, repeated every 4 weeks. The recommended dose of this regimen had been previously determined as irinotecan at a dose of 50 mg/m^2 and docetaxel at a dose of 30 mg/m^2 in a phase 1 study at our institution.[25] Of the 12 patients, 3 had been recruited in this phase 1 study and the other 9 were treated with ID in clinical practice after the recommended dose had been determined. A median of 3 cycles of ID were given, ranging from 1 to 6 cycles. In the 7 patients with locoregional disease and no prior radiotherapy, the treatment plan called for ID followed by definitive radiotherapy. Radiotherapy was administered after a median of 3 cycles of ID (range, 1–6 cycles). One patient refused further administration of ID because his nasal bleeding was not improved after 1 cycle and he wished to receive definitive radiotherapy as soon as possible. A second patient received 6 cycles of ID because she wished to continue ID as long as a response was observed. The other 5 patients received 2 or 3 cycles of ID. Of the 7 patients, the 1 patients with Kadish stage B disease underwent definitive radiotherapy with photon radiation (total of 66 grays [Gy] in 2-Gy fractions), whereas the 6 patients with Kadish stage C disease received proton radiation (total of 65 cobalt Gray equivalents [GyE] in 2.5-GyE fractions).

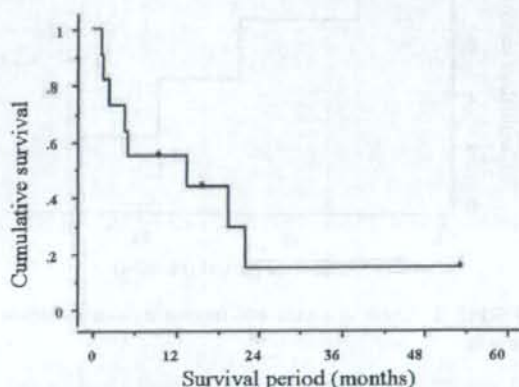All 12 patients demonstrated an assessable response to ID. Three of the 12 achieved a partial

FIGURE 1. Progression-free survival (n = 12).

response (PR). One PR patient had distant metastatic disease and the other 2 PR patients had locoregional disease. The median progression-free survival was 13.6 months (range, 1.3–53.4 months) (Fig. 1). In the 7 patients with locoregional disease and no prior radiotherapy who received definitive radiotherapy after chemotherapy, 5 achieved a CR and 2 a PR.

The median follow-up period in survivors was 22.2 months (range, 14.8–63 months). Estimated 1-year and 2-year survival rates were 83.3% and 53.3%, respectively. The median overall survival was 36.6 months (Fig. 2). The median survival of the 6 of 12 patients with recurrent or distant metastatic disease was 16.1 months (Fig. 3). Of the 7 of 12 patients with locoregional disease who had received no prior
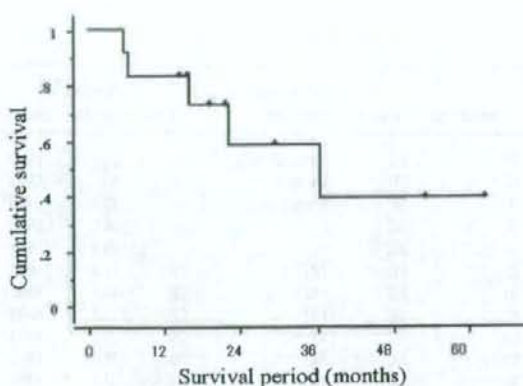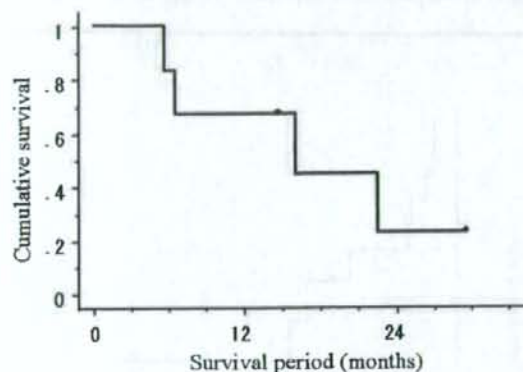
FIGURE 2. Overall survival (n = 12).

FIGURE 4. Survival in patients treated with irinotecan plus docetaxel followed by definitive radiation therapy (n = 7).

FIGURE 3. Survival in patients with recurrent or metastatic disease (n = 6).

TABLE 2
Response According to Patient Characteristics

Characteristic	No.	No. of patients responding	P
Age <50 y	4	3	.018
Age ≥50 y	8	0	
Male	4	1	>.99
Female	8	2	
Distant metastasis			>.99
Present	3	1	
Absent	9	2	
Kadish stage B	2	0	>.99
Kadish stage C	10	3	
Intracranial invasion			.045
Present	5	3	
Absent	7	0	
Low Hyam grade (I/II)	2	0	>.99
High Hyam grade (III/IV)	8	3	

radiotherapy, 1 received ID followed by photon radiation and 6 received ID followed by proton radiation. Among them, the 2-year survival rate was 100% and 6 patients were alive at the time of last follow-up (Fig. 4). Of the 5 CR patients who received definitive radiotherapy (1 with photon radiation and 4 with proton radiation), 4 patients were alive at the time of last follow-up with no evidence of disease. Toxicity of definitive photon or proton radiotherapy was mild and manageable. None of the 7 patients experienced treatment-related death or severe late toxicity due to irradiation, including vision impairment, brain necrosis, or others. Nevertheless, ongoing follow-up to ensure safety is required.

The most common grade 3 or 4 chemotherapy-related toxicities were leukopenia (33%), neutropenia (50%), febrile neutropenia (8%), and diarrhea (25%), all of which were manageable.
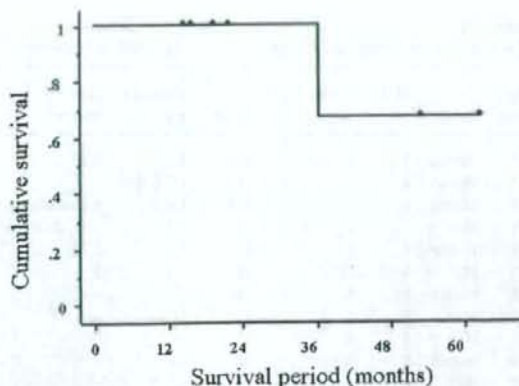
The correlation between response to chemotherapy and clinical and histologic variables is summarized in Table 2. The response rate to ID was 75% (3 of 4 patients) in the group aged <50 years, but was 0% (0 of 8 patients) in those aged >50 years ($P = .018$). Furthermore, the response rate was 60% (3 of 5 patients) in patients with intracranial invasion, but was 0% (0 of 7 patients) in those without ($P = .045$). Although the sample size was small, no response was observed (0 of 2 patients) in the Hyams low-grade (grade I/II) patients, whereas 3 responses were observed (3 of 8 patients) in the Hyams high-grade (grade III/IV) patients. No significant correlations between response to chemotherapy and other clinical variables were identified.

DISCUSSION

As ONB is a rare tumor, and to our knowledge no consensus exists regarding treatment, particularly for advanced cases. Review of the literature suggests that ONB is a surgical disease; the advent of craniofacial resection has clearly improved disease-free survival[6,15] and many authors recommend surgery as the initial treatment.[8,12,31,32] To improve locoregional control and survival, several authors recommend surgery followed by adjuvant radiotherapy.[10,12,31–33] Together, these reports suggest that the optimal treatment for surgically resectable cases is surgery followed by adjuvant radiotherapy.

Of our 12 patients with ONB, 5 had recurrent disease, 3 had intracranial invasion, 1 each had cervical lymph node metastases and distant metastases, and 2 were staged as Kadish B. Because these Kadish stage B patients declined surgery, treatment was initiated with chemotherapy and, if the disease was locoregional, continued with definitive radiotherapy after chemotherapy with ID.

Many authors have commented on the effectiveness of chemotherapy in the treatment of ONB.[7,12,14,18,19,34–37] Notwithstanding that these previous reports were based on single-institution experience with relatively small sample sizes, platinum-based chemotherapy was well regarded and considered effective.[14,36,37] We previously reported that 2 of 8 ONB patients responded to chemotherapy with mainly platinum-based regimens.[23] In our present analysis in 12 patients treated with ID, the response was also 25% (3 of 12 patients), but toxicities were mild and manageable. The median survival in the setting of recurrent or metastatic disease was approximately 12 months in previous reports,[22,31] but was 16.1 months in the current study. Although our sample size was small (n = 6), this result might indicate that chemotherapy for recurrent or metastatic ONB contributes to improving survival.

On univariate analysis, response rates to ID were significantly higher in patients aged <50 years and those with intracranial invasion. Rates for high-grade (Hyams grade III/IV) and low-grade (Hyams grade I/II) ONB were 37.5% (3 of 8 patients) and 0% (0 of 2 patients), respectively, but this difference was not statistically significant. Several authors have reported that the pathologic features of ONB correlate with its prognosis and response to chemotherapy,[1,10,18,26–28] whereas McElroy et al.[18] suggested that high-grade ONB (Hyams grade III/IV) may be sensitive to chemotherapy. Data from the current study may also suggest that ONB in younger patients and in those with aggressive disease extension may be sensitive to chemotherapy. The question of which subset of ONB

patients will respond to chemotherapy is important but remains to be answered. The ability to predict response will allow the identification of those patients who should receive chemotherapy before definitive radiotherapy. Our present and previous reports may suggest that younger patients, those with aggressive disease extension, and those with high-grade histology (Hyams grade III/IV) may be sensitive to chemotherapy.[1,10,18,26–28] ONB is a rare disease, and identification of the clinical determinants of a response to chemotherapy will require further accumulation of patients.

Although craniofacial resection is effective in controlling ONB, it is not without substantial risk and morbidity. Levine et al.[38] reported that of 27 patients undergoing this treatment, 20% experienced cerebrospinal fluid leakage and 12% had symptomatic postoperative pneumocephalus. Similarly, Richtsmeier et al.[39] reported 1 death and 9 major intracranial complications among a total of 26 patients. Radiotherapy as the initial treatment has been proposed as 1 means of obviating these complications. Elkon et al.[2] found that radiotherapy and surgery provided equivalent results in patients with early-stage disease. Similarly, a review from the Mayo Clinic indicated no significant difference in survival between patients receiving either radiotherapy or surgery alone.[10] However, recurrence with radiotherapy alone was approximately 60%.[2,33] Bhattacharyya et al.[13] reported excellent results in 9 cases of esthesioneuroblastoma (olfactory neuroblastoma) or neuroendocrine carcinoma treated using induction chemotherapy with cisplatin and etoposide followed by proton radiotherapy, with 8 of 9 patients exhibiting a dramatic response to therapy and remission of their tumor, which obviated the need for resection. Fitzek et al.[14] also reported promising results with the combination of induction chemotherapy and proton-photon radiotherapy for patients with advanced ONB. Nineteen patients with a sinonasal tumor (10 olfactory neuroblastoma and 9 neuroendocrine carcinoma) received chemotherapy with 2 courses of cisplatin and etoposide, followed by high-dose proton-photon radiotherapy to 69.2 GyE. Thirteen of the 19 responded to chemotherapy, with a 5-year survival rate of 74% and 5-year local control rate from the time of initial treatment of 88%. These findings demonstrated the possibility of nonsurgical treatment for ONB.

Nevertheless, radiotherapy for ONB is challenging because of the surrounding critical organs, including the optic pathway, brain, and brainstem. Thanks to its physical characteristics, proton radiotherapy provides better dose distribution than